"Waves on density interfaces"

Peter Davies
(University of Dundee, UK)

Waves on interfaces

- Density interfaces within water column

- Variations in temperature, solute concentration and/or suspended material

-

Waves on interfaces

- Density interfaces within water column
- Variations in temperature, solute concentration and/or suspended material
- Water column stably-stratified
- Examples: Lakes, reservoirs, shelf seas, coastal zones, deep ocean, estuaries etc etc

Waves on interfaces

- Density interfaces within water column
- Variations in temperature, solute concentration and/or suspended material
- Water column stably-stratified
- Examples: Lakes, reservoirs, shelf seas, coastal zones, deep ocean, estuaries etc etc

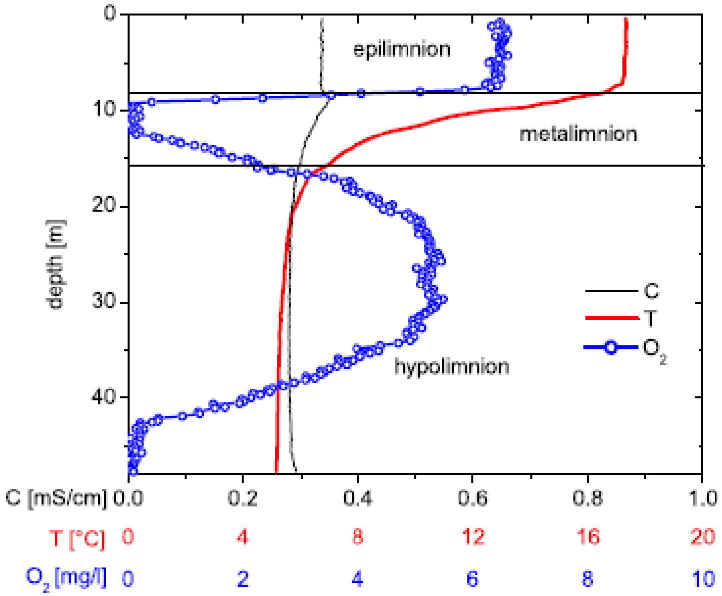

Figure 7. Profiles of temperature (T), (in situ) conductivity (C), and concentration of dissolved oxygen (O_2) from 6 September 2000 in Arendsee, Germany (adapted from *Boehrer and Schultze* [2005] with permission from ecomed). The boundaries between layers were drawn along gradients in oxygen profiles. (Oxygen concentration numerically corrected for response time of 7.5 s of sensor.)

Waves on Interfaces: internal waves

- First “laboratory” observations
- *Italian lamp*: thick layer of oil floating on thick layer of water, with improvised cork and wick

- Benjamin Franklin, 1762

Waves on Interfaces: internal waves

- First “laboratory” observations
- *Italian lamp*: thick layer of oil floating on thick layer of water, with improvised cork and wick
- ".. tho’ the surface of the oil was perfectly tranquil, and duly preserved its position and distance with regard to the brim of the glass, the water under the oil was in great commotion rising and falling in irregular waves”
- Benjamin Franklin, 1762

Internal waves on interfaces

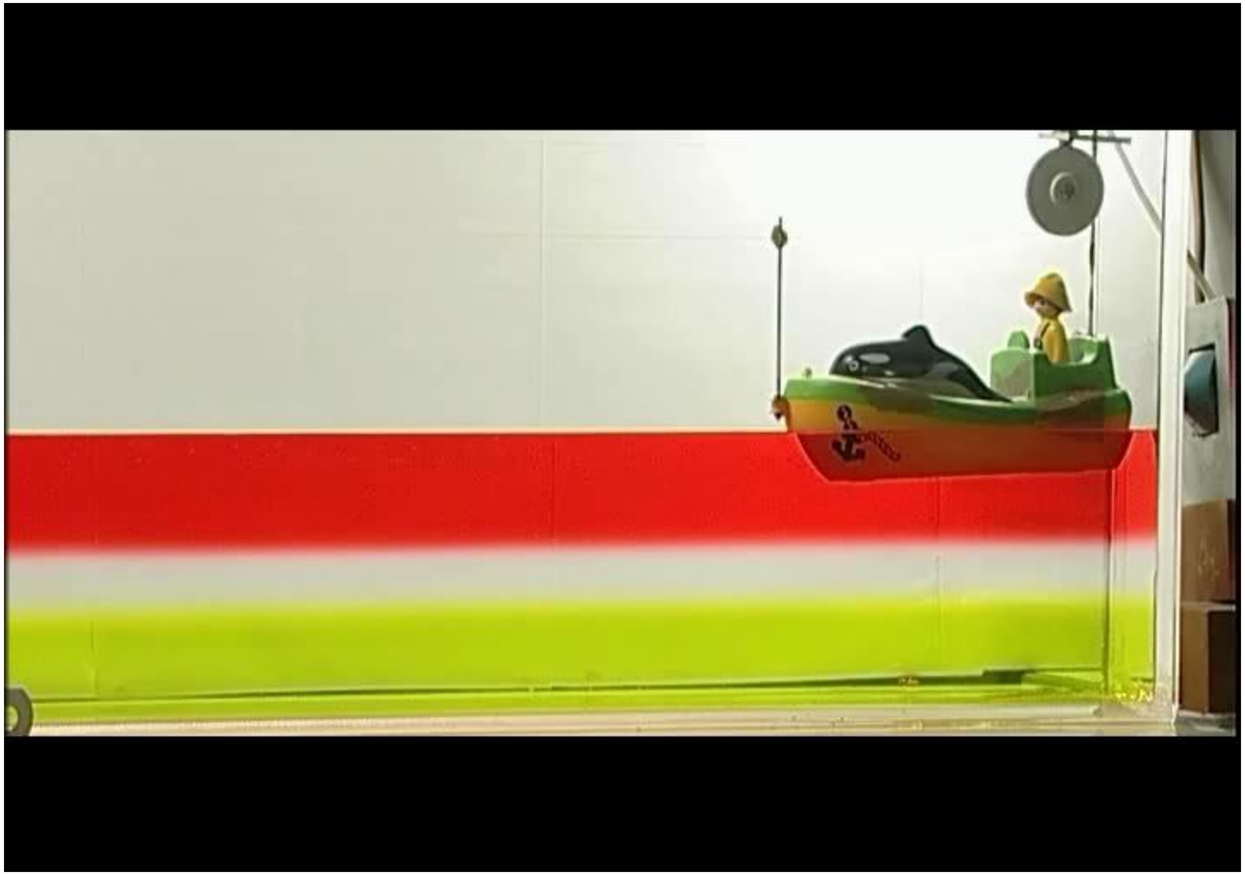

Courtesy: Thierry Dauxois (Ecole Normale Supérieure de Lyon)

Internal Solitary Waves (ISWs)

- NONLINEAR Waves of permanent form
- Balance between nonlinearity & dispersion

- 90% of K.E of nonlinear baroclinic modes contained within modes 1 and 2

Internal Solitary Waves (ISWs)

- NONLINEAR Waves of permanent form
- Balance between nonlinearity & dispersion
- 90% of K.E of nonlinear baroclinic modes contained within modes 1 and 2
- Mode 1: waves of depression (elevation) with no peak (trough)
- Isopycnals displaced in one direction

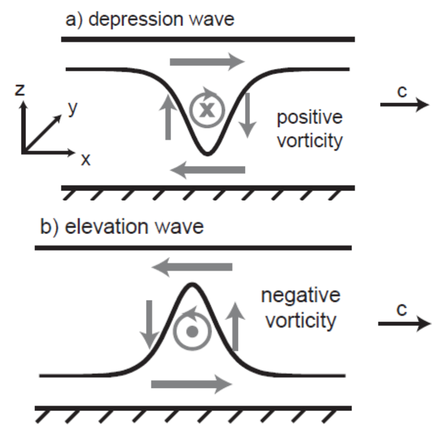

Internal Solitary Waves (ISWs)

- NONLINEAR Waves of permanent form
- Balance between nonlinearity & dispersion

- 90% of K.E of nonlinear baroclinic modes contained within modes 1 and 2

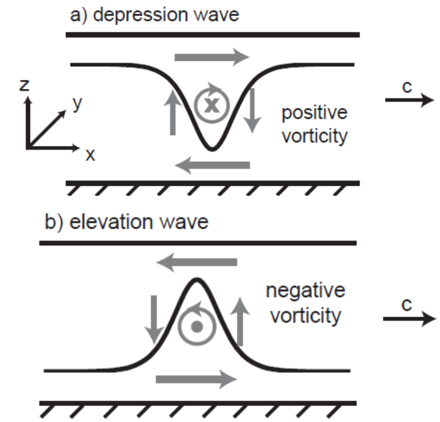

- Mode 1: waves of depression (elevation) with no peak (trough)
- Isopycnals displaced in one direction

- Mode 2: "varicose" or "bulge" waves
- Upper and lower isopycnals displaced in opposite directions

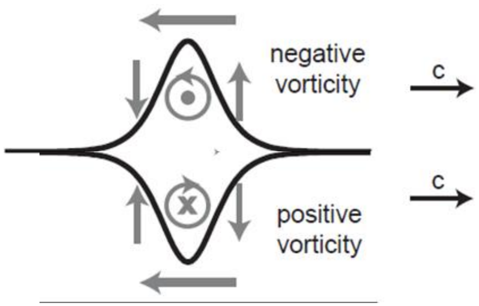

Internal Solitary Waves (ISWs)

- Occurrence

- Lakes
- Relaxation of wind stress
- Basin scale seiching $\rightarrow$ transfer to shorter length scales
- Steepening of waves $\rightarrow$ packets of ISWs $\rightarrow$ boundary mixing
- Flux path from wind to turbulent benthic boundary layer

Internal Solitary Waves (ISWs)

- Occurrence

- Lakes
- Relaxation of wind stress
- Basin scale seiching → transfer to shorter length scales
- Steepening of waves → packets of ISWs → boundary mixing
- Flux path from wind to turbulent benthic boundary layer

- River plumes
- Rapid deceleration → packets of ISWs

- Estuaries, Waterways

Internal Solitary Waves (ISWs)

- Occurrence

- Lakes
- Relaxation of wind stress
- Basin scale seiching → transfer to shorter length scales
- Steepening of waves → packets of ISWs → boundary mixing
- Flux path from wind to turbulent benthic boundary layer

- River plumes
- Rapid deceleration → packets of ISWs

- Estuaries, Waterways

- Shelf Seas, Coastal zones, Deep ocean - (tidal forcing)

ISWs Mode 1 – Lake observations

- Lake Constance/Bodensee
- (Preusse, Peeters & Lorke, *Limnol. Oceanog*. (2010))

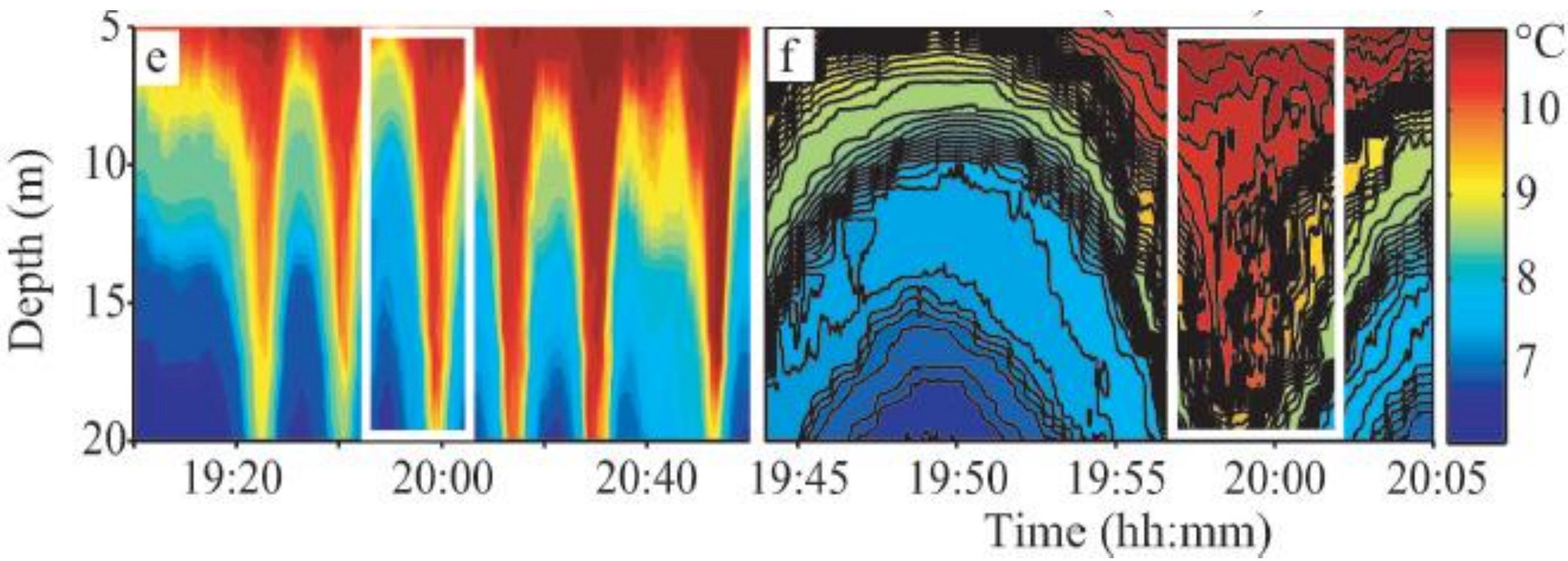

Isotherm displacements (15-20m)

Oceanographic ISWs: Mode 1

- Ship-borne measurements
- Mode 1 ISWs of depression

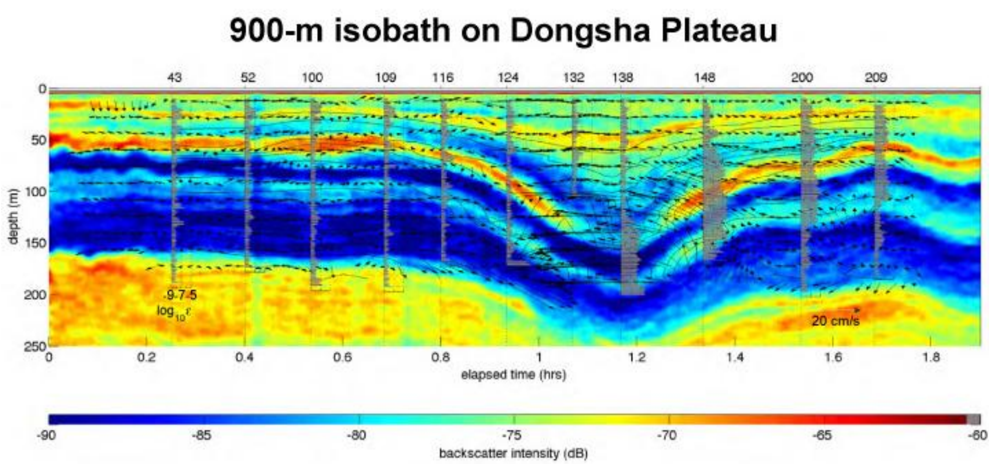

Backscatter from 120 kHz Simrad EK500, ADCP data from shipboard 150 kHz RDI system.
In-situ measurements with microstructure profiler.

~100 m displacement

http://www.whoi.edu/science/PO/turbulence/Fieldwork/south_china_sea.php

Oceanographic ISWs: Mode 1

- Ship-borne measurements
- Mode 1 ISWs of depression

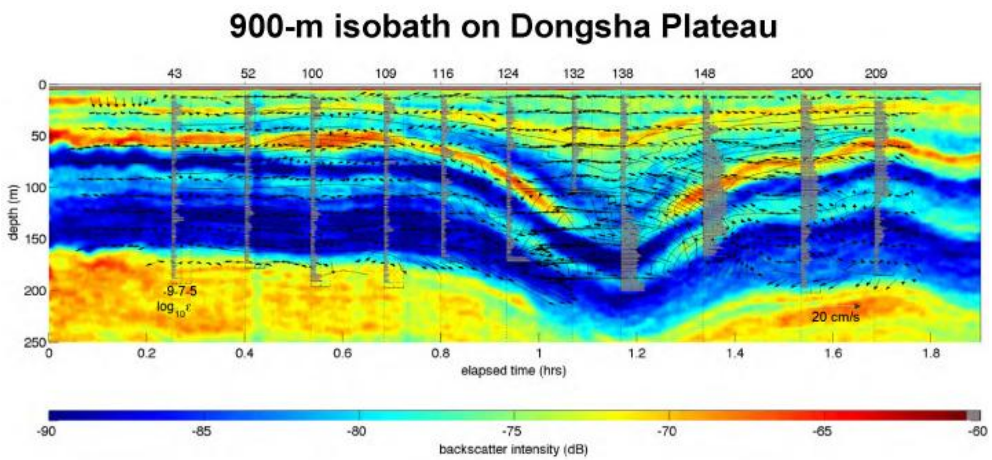

Backscatter from 120 kHz Simrad EK500, ADCP data from shipboard 150 kHz RDI system.
In-situ measurements with microstructure profiler.

~100 m displacement

http://www.whoi.edu/science/PO/turbulence/Fieldwork/south_china_sea.php

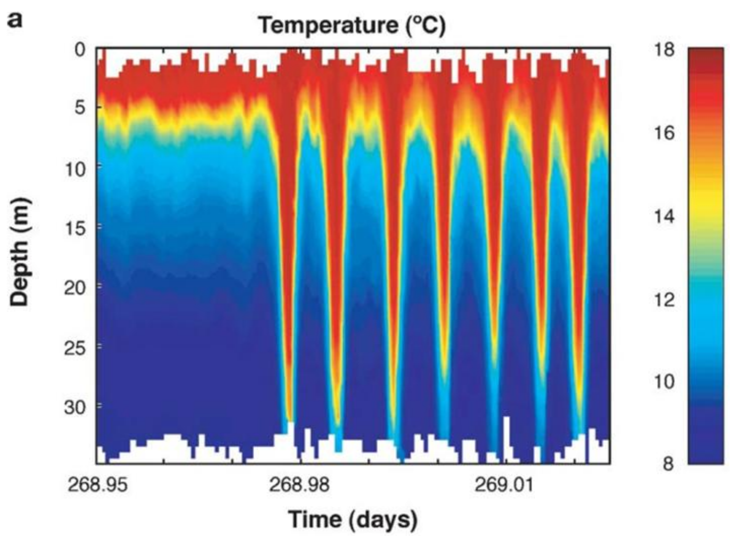

~30 m displacement

Stanton & Ostrovsky, 1998: Oregon Shelf

Synthetic Aperture Radar (SAR) observations

- ISW-induced regions of surface convergence, divergence
- Surface roughness anomalies

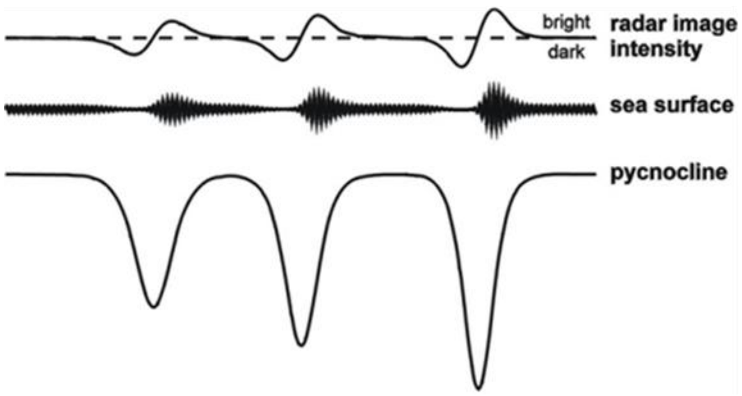

Packet of Mode-1 waves of depression

Synthetic Aperture Radar (SAR) observations

- ISW-induced regions of surface convergence, divergence
- Surface roughness anomalies

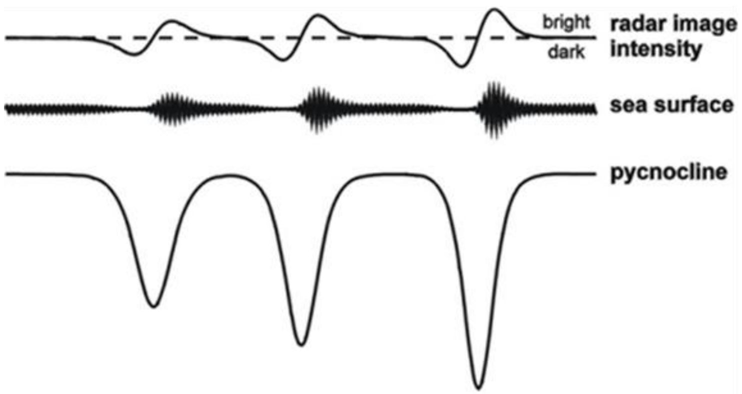

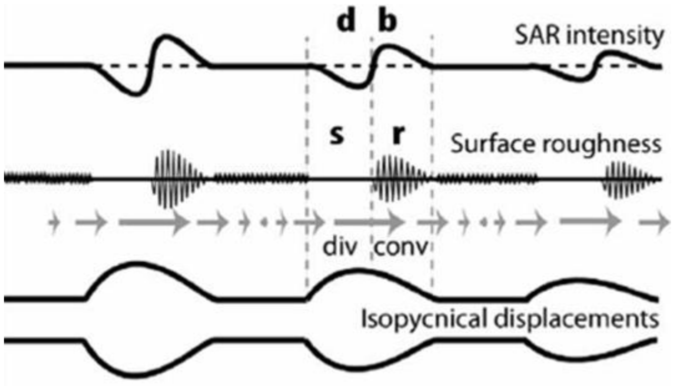

Packet of Mode-1 waves of depression

Mode-2 ISW

Oceanographic ISWs: Mode 1

- SAR observations [*e.g* Apel 2002][1]

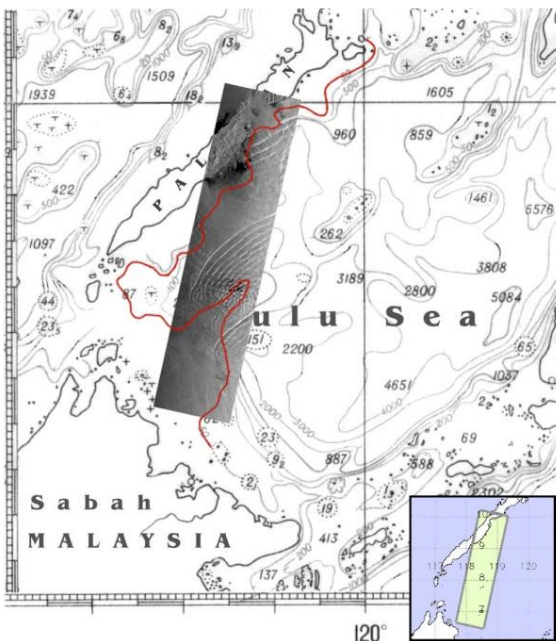

Sulu Sea

Andaman Sea

Apel, J.R. (2002) Oceanic internal waves and solitons. In ***An Atlas of Oceanic Internal Solitary Waves***, Global Ocean Associates, Washington DC, USA.

Oceanographic ISWs: Mode 1

- Rank-ordered (amplitude) wave packets
- High induced currents/vertical shear
- Celerity ~ 8 km per hour

- Duda *et al* (2004): amplitude 150 m in water depth of 340 m in S China Sea

- Van Gastel *et al* (2009): 83 m in 124 m depth (NW Australia)

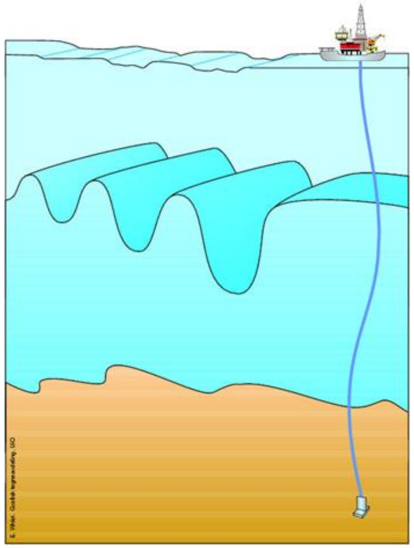

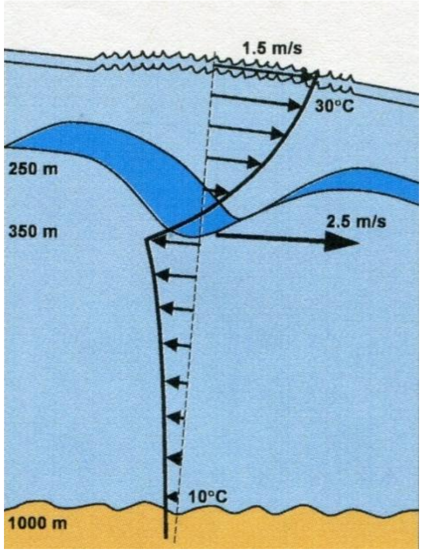

Oceanographic ISWs: Mode-1 Effects

- Rig tilting: 3-5°
- Displacements: >4 m (V), >200 m (H)

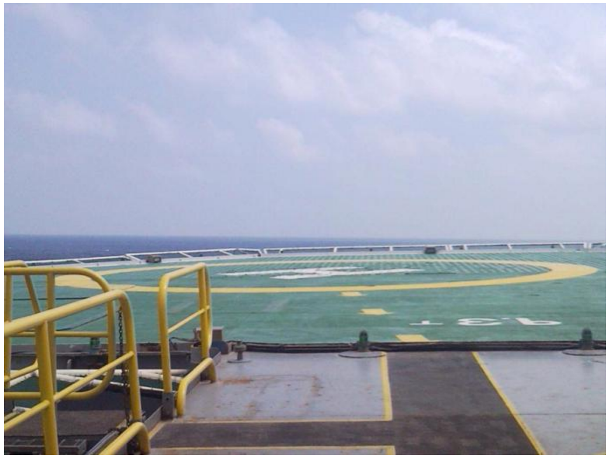

ISW- tilted helipad (AFTER appropriate action)
Previous displacement 189m, broken drill string

Oceanographic ISWs: Mode-1 Effects

- Rig tilting: 3-5°
- Displacements: >4 m (V), >200 m (H)
- Stresses on drill pipes; drill string breakages; drilling down time 10d/a, fatigue damage to moorings, risers
- Anchor chains parting
- Supply vessels forced into rigs, ROVs lost

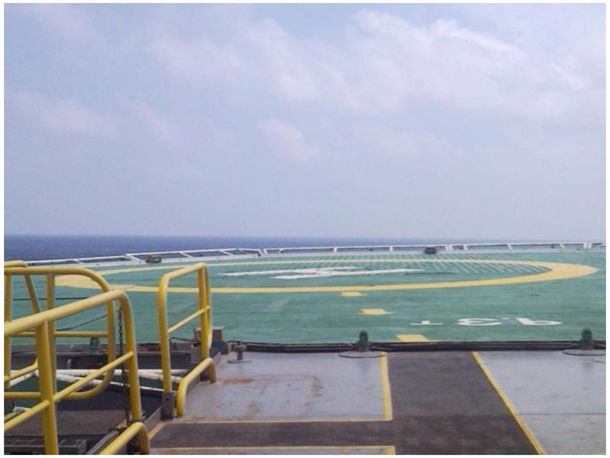

ISW- tilted helipad (AFTER appropriate action)
Previous displacement 189m, broken drill string

Oceanographic ISWs: Mode-1 Effects

- Rig tilting: 3-5°
- Displacements: >4 m (V), >200 m (H)
- Stresses on drill pipes; drill string breakages; drilling down time 10d/a, fatigue damage to moorings, risers
- Anchor chains parting
- Supply vessels forced into rigs, ROVs lost
- USD$ M rig repositioning costs for excessive rig listing

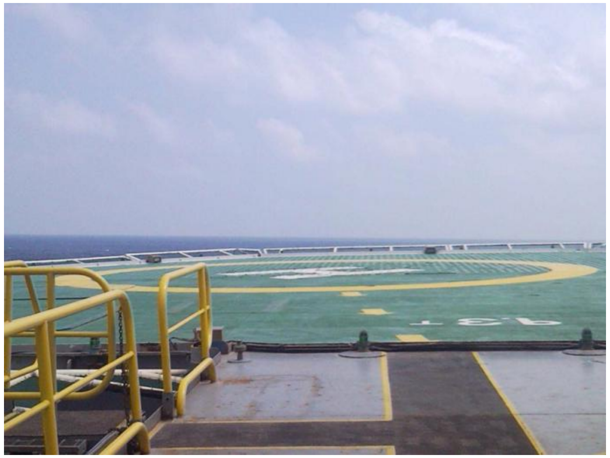

ISW- tilted helipad (AFTER appropriate action)
Previous displacement 189m, broken drill string

Laboratory Modelling: Mode 1 ISWs

- Experimental tank: (*e.g* Carr & Davies, PoF, 2006)

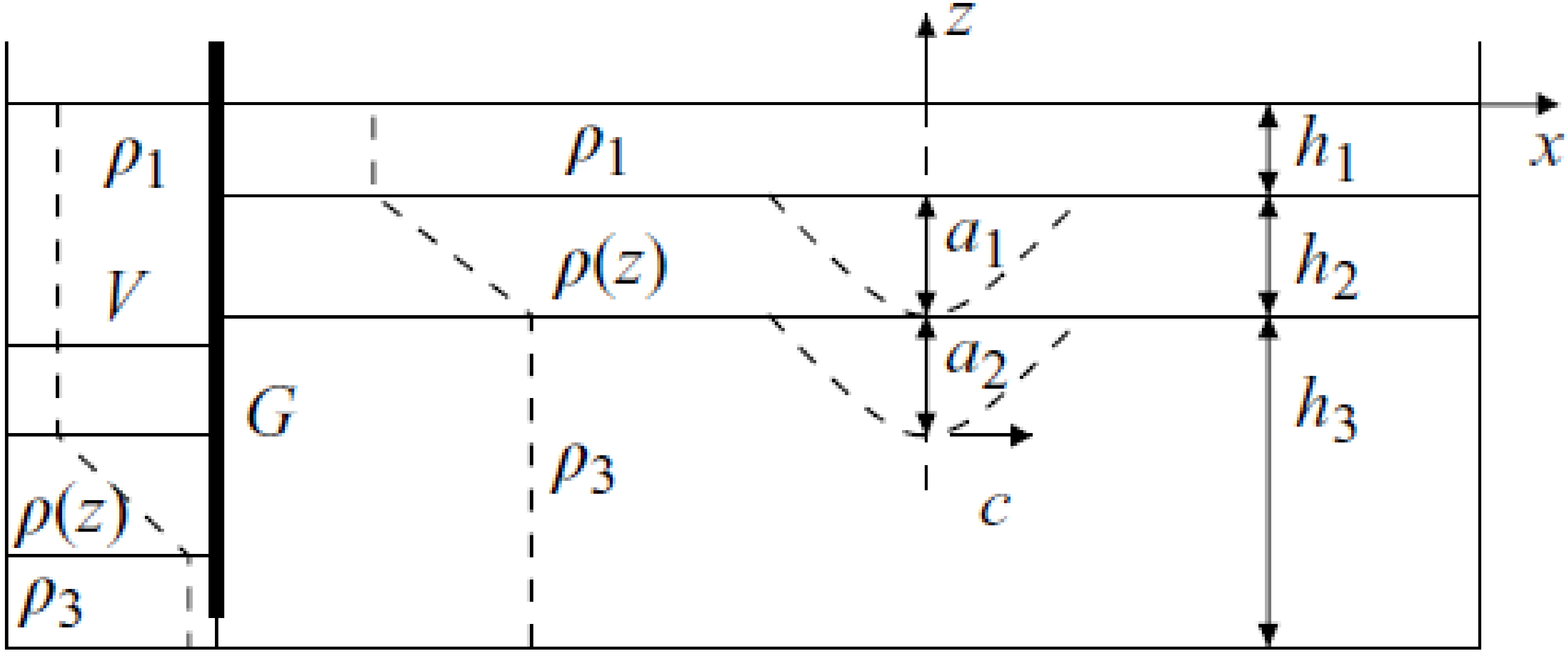

Mode 1 ISW:

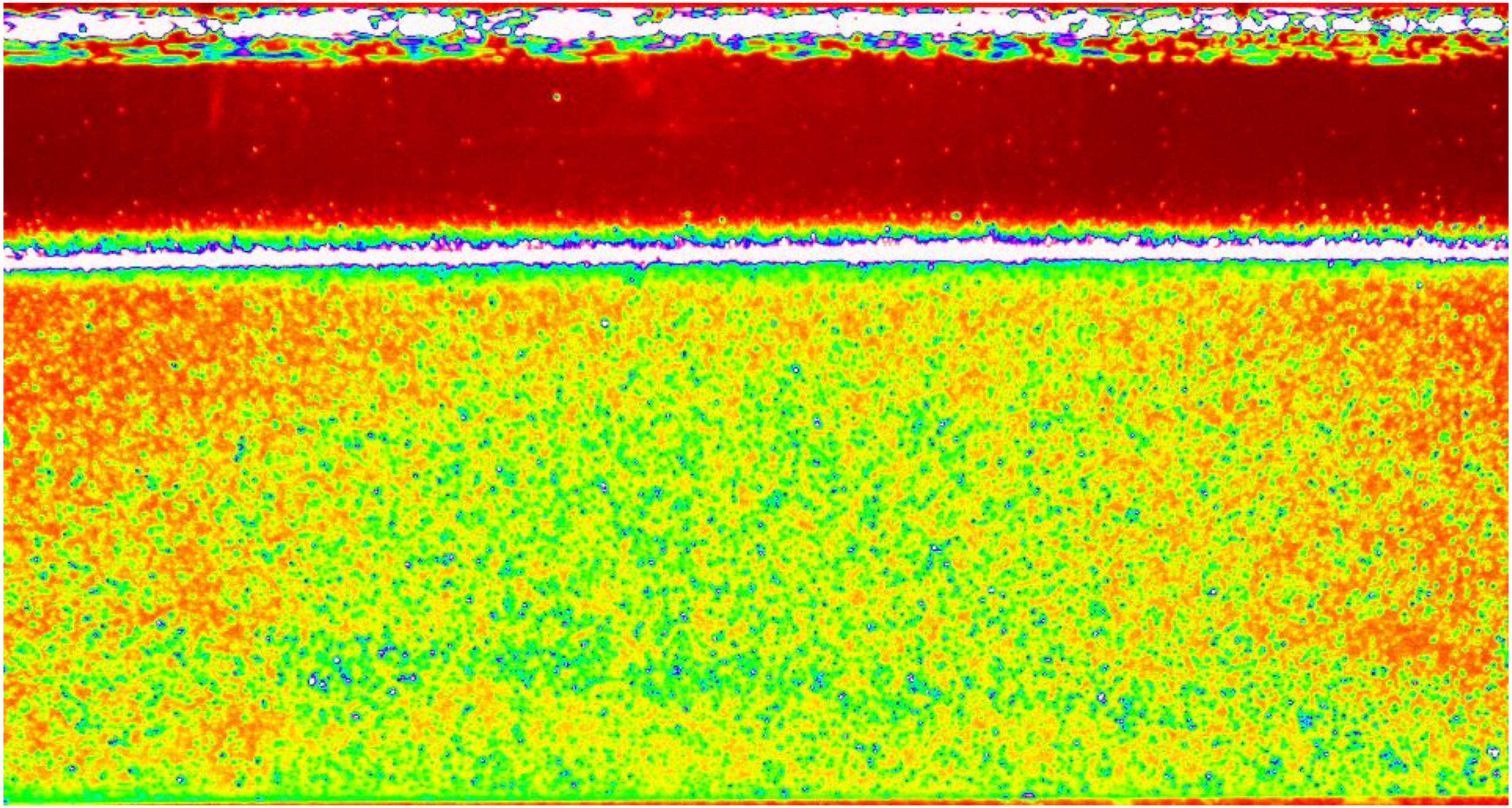

Boundary jet – Mode 1 ISW (depression)

- PIV Results (Carr & Davies, PoF, 2006)
- Residual velocity *u* (*z*) behind the wave peak at $x = x_0$

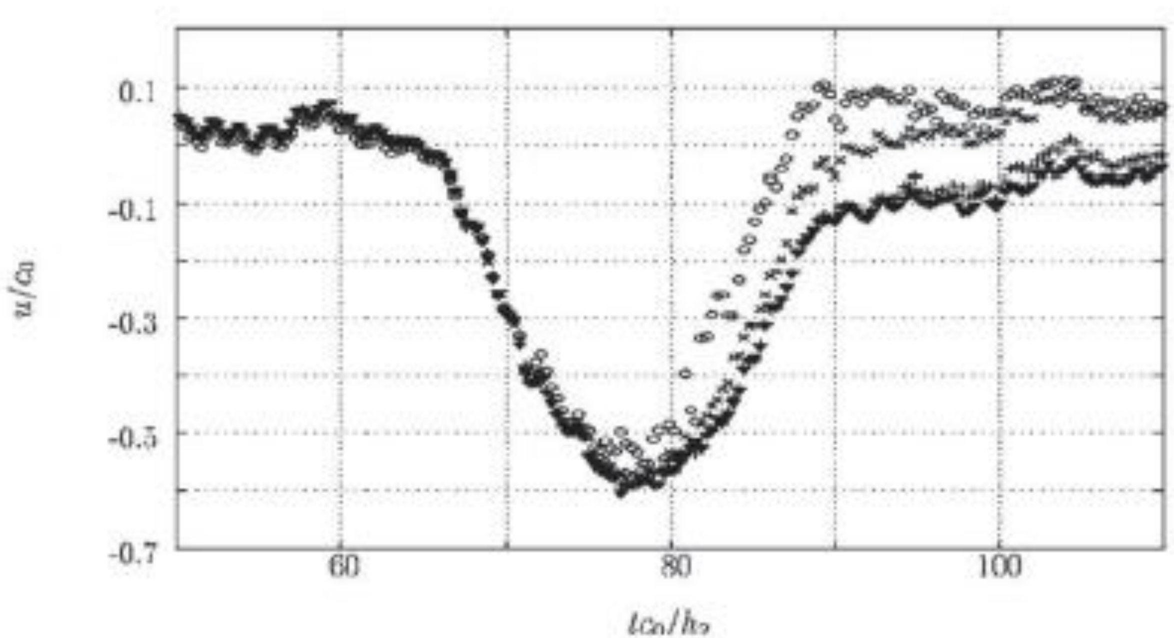

← $u/c_0 = 0$

Time series plots of u/c_0 versus tc_0/h_2 at z/h_2 = (o) 0.1, (x) 0.2, (+) 0.4

c_0 = linear phase speed, h_2 = layer thickness

Boundary jet

- Comparisons with Bergen Ocean Model (BOM)

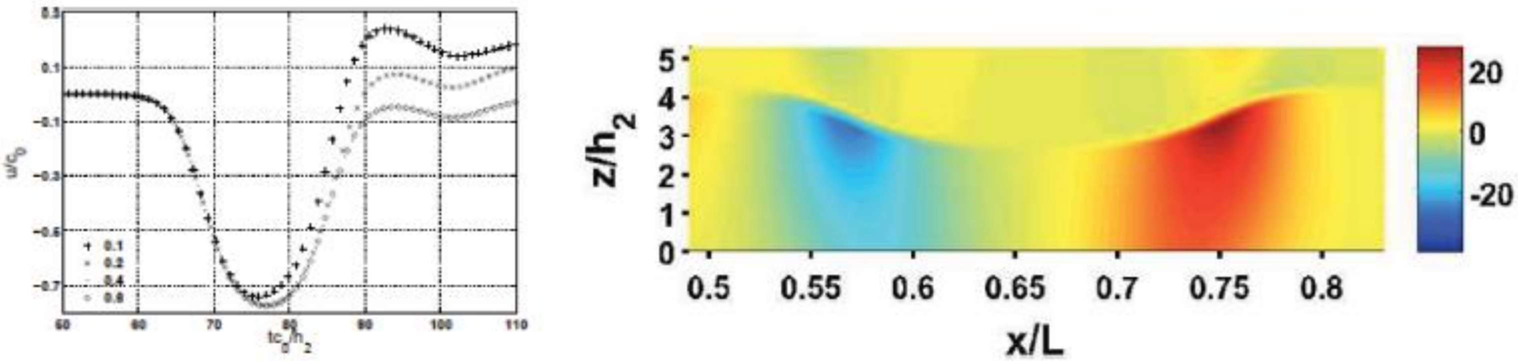

Figure 4 BOM (see text) simulations of Carr and Davies (2006) experiments for ISWs of depression (see Fig 3a), showing (a) u/c_0 versus tc_0/h_2 at various z/h_2 (see legend) and (b) horizontal (x) pressure gradients $\Delta p/\rho_2 c_0^2 L$ beneath the wave In (b) positive (negative) values of $\Delta p/\rho_2 c_0^2 L$ indicate increasing pressure to the right (left). From Thiem *et al.* (2011).

Mode 1 ISW, boundary jet instability

Carr, Davies & Shivaram, PoF, 2008

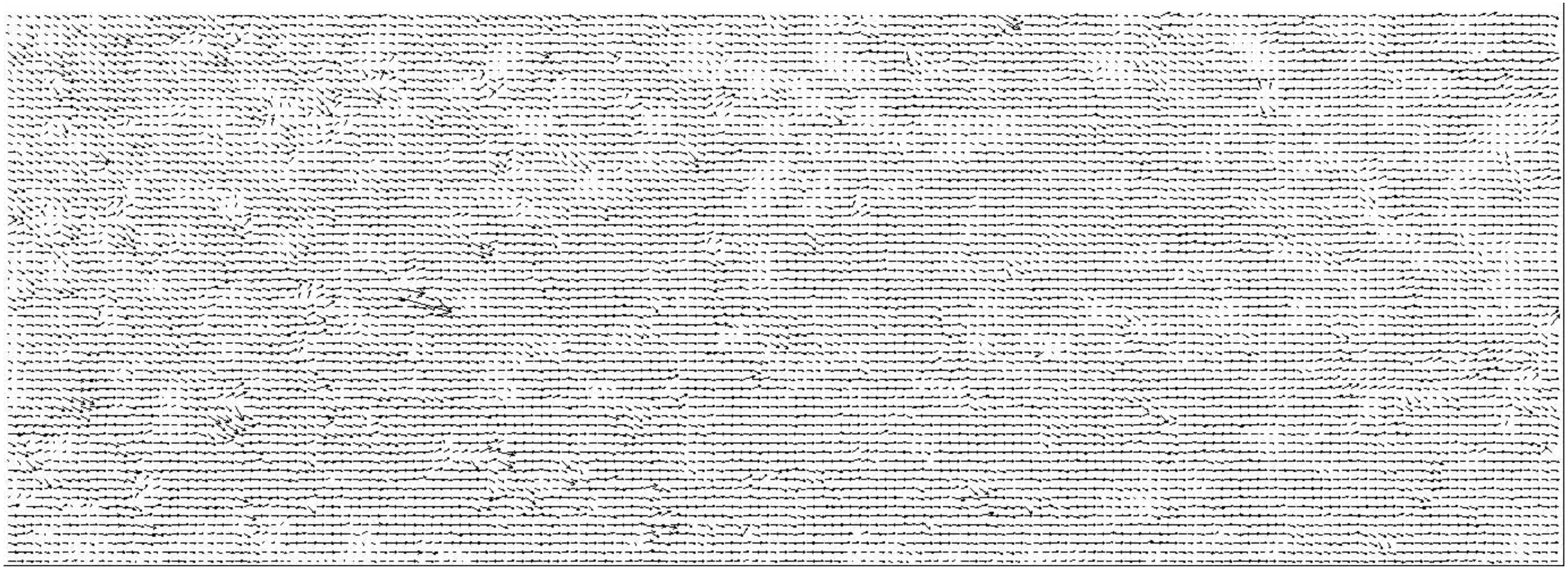

Mode 1 ISW: sediment suspension

Aghsahee *et al*, JFM, 2012

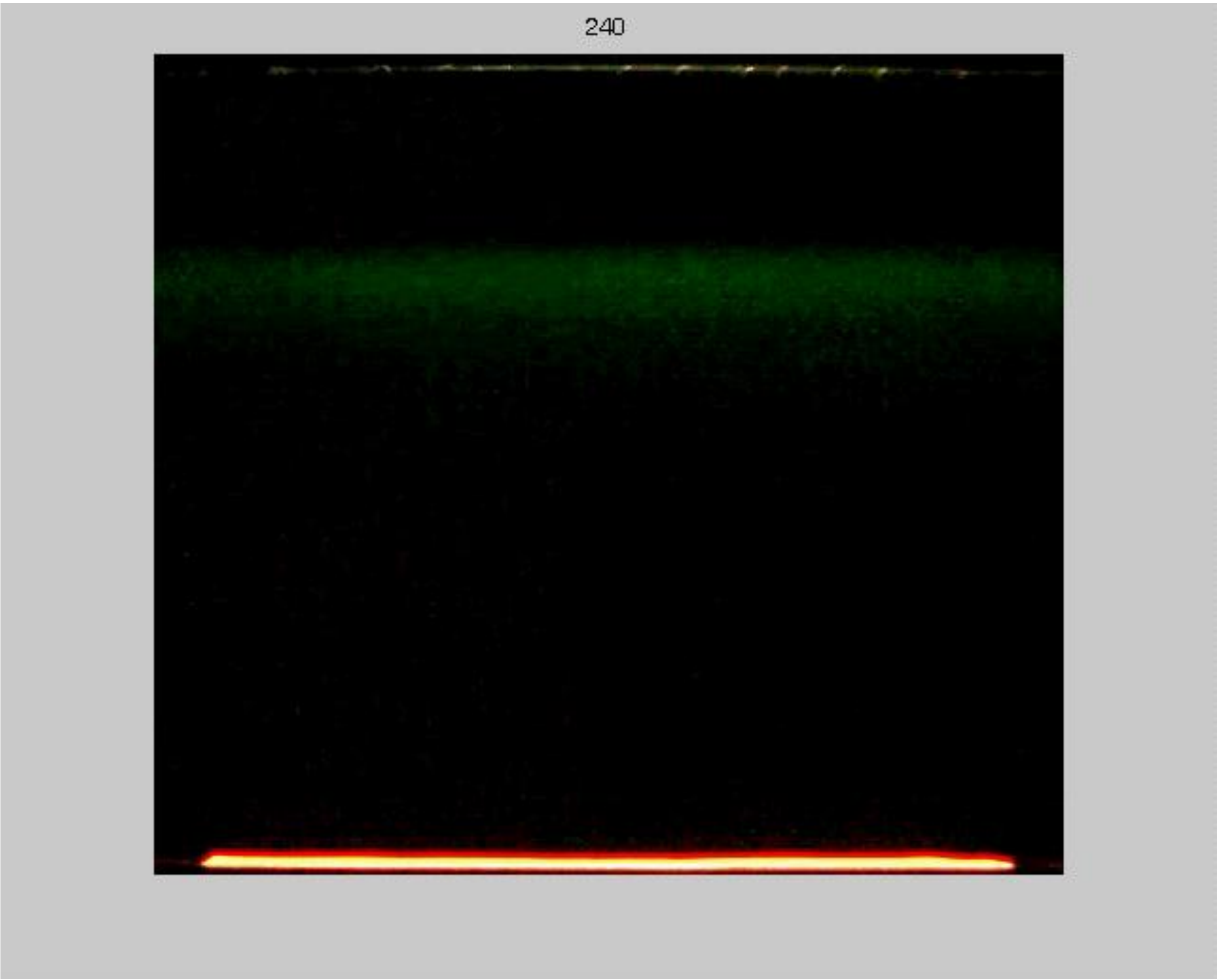

Mode 1: Wave breaking

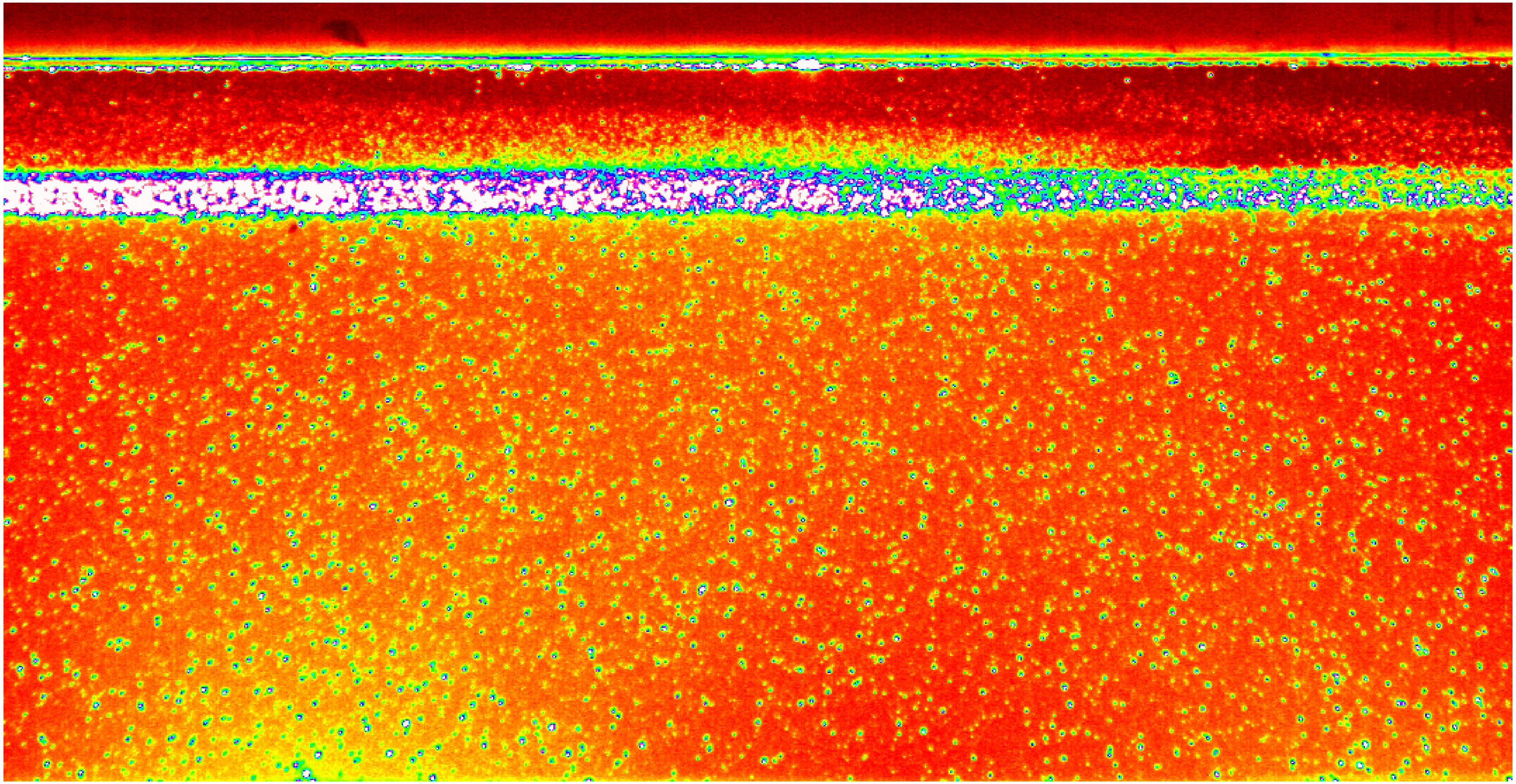

ISW breaking

- Shear instability?
- Define: $Ri_g = [g(\partial \rho/\partial z)]/[\rho_0(\partial u/\partial z)^2]$
- Linear stability condition (parallel shear flow): $Ri_g < (1/4)$

ISW breaking

- Shear instability?
- Define: $Ri_g = [g(\partial\rho/\partial z)]/[\rho_0(\partial u/\partial z)^2]$
- Linear stability condition (parallel shear flow): $Ri_g < (1/4)$

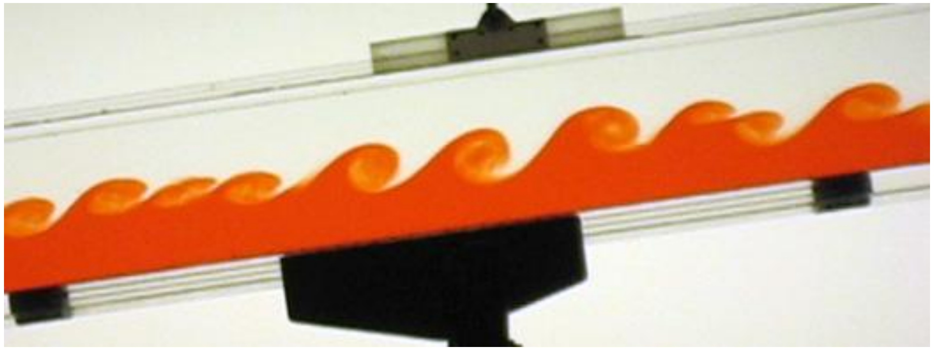

ISW breaking

- Shear instability?
- Define: $Ri_g = [g(\partial\rho/\partial z)]/[\rho_0(\partial u/\partial z)^2]$
- Linear stability condition (parallel shear flow): $Ri_g < (1/4)$

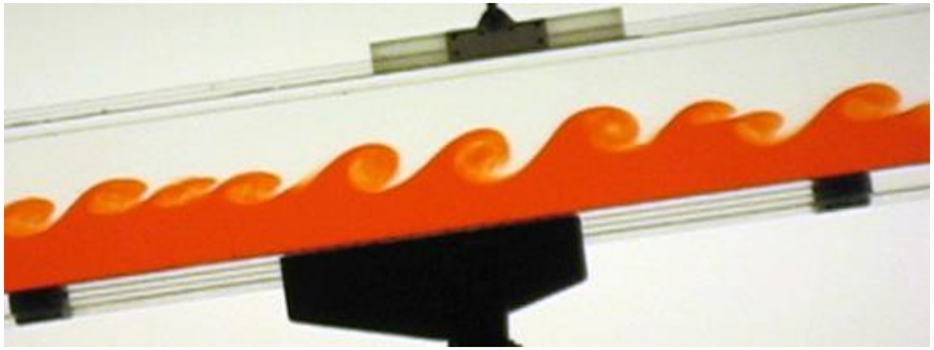

Mode-1 ISWs

- Laboratory Modelling: Wave breaking
- Dalziel, Carr, Sveen & Davies (2007) Meas. Sci. & Tech., 18, 533-547
- Fructus, Carr, Grue, Jensen & Davies (2009) JFM, 620, 1-29
- Carr, Fructus, Grue, Jansen & Davies (2008) PoF, 20, 126601

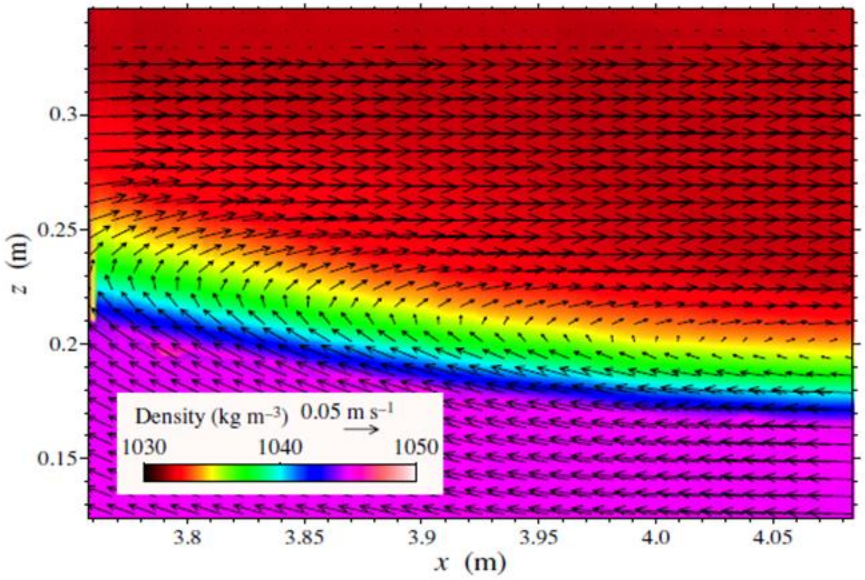

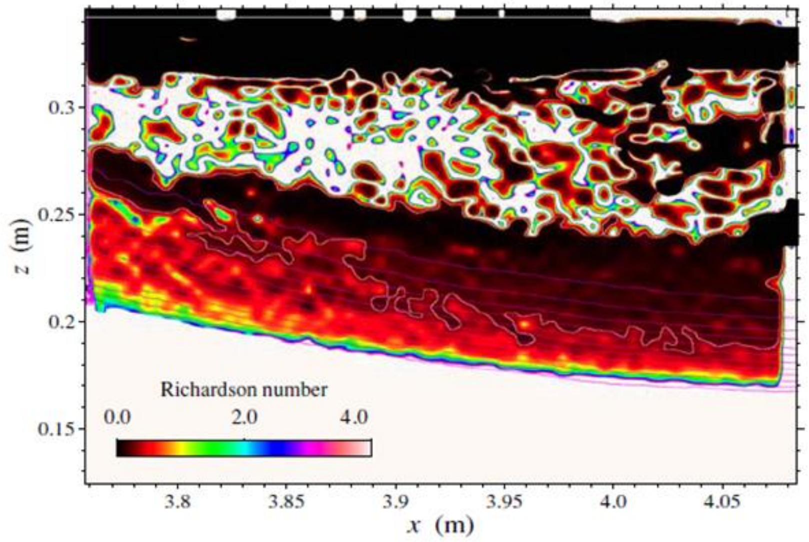

Figure 13. The gradient Richardson number (false colour) with contours of density superimposed in magenta at intervals of 1 kg m^{-3} from $\rho = 1033$ kg m^{-3} to $\rho = 1044$ kg m^{-3} (top to bottom). The $Ri = 1/4$ contour is highlighted in white.

Mode 1 ISWs: Theoretical model

- Grue *et al*, JFM, 1999

- Solid – fully nonlinear solution
- Dash – Korteweg de Vries solution

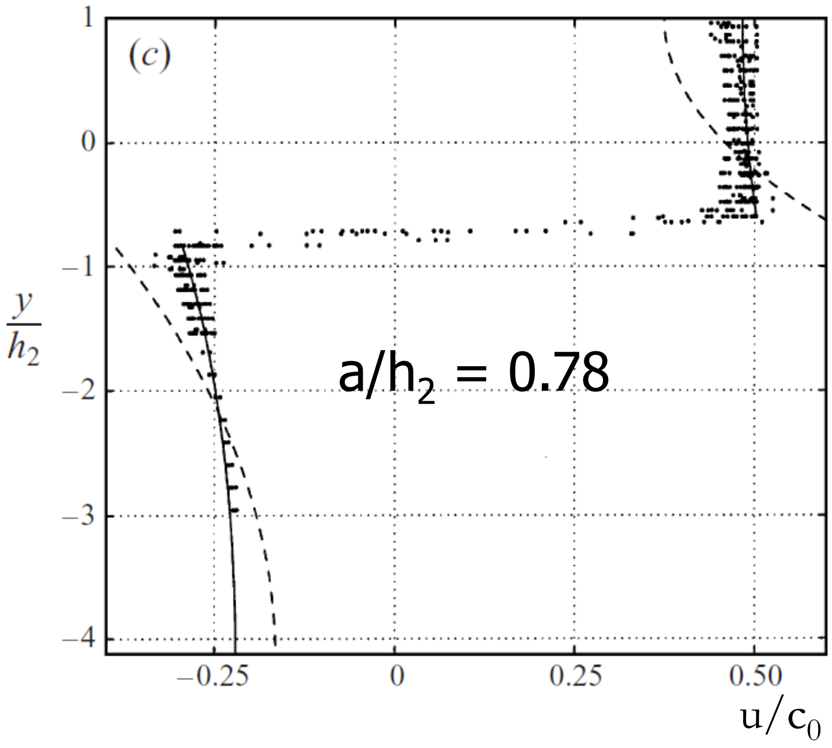

Comparisons: lab data & theory

- No breaking

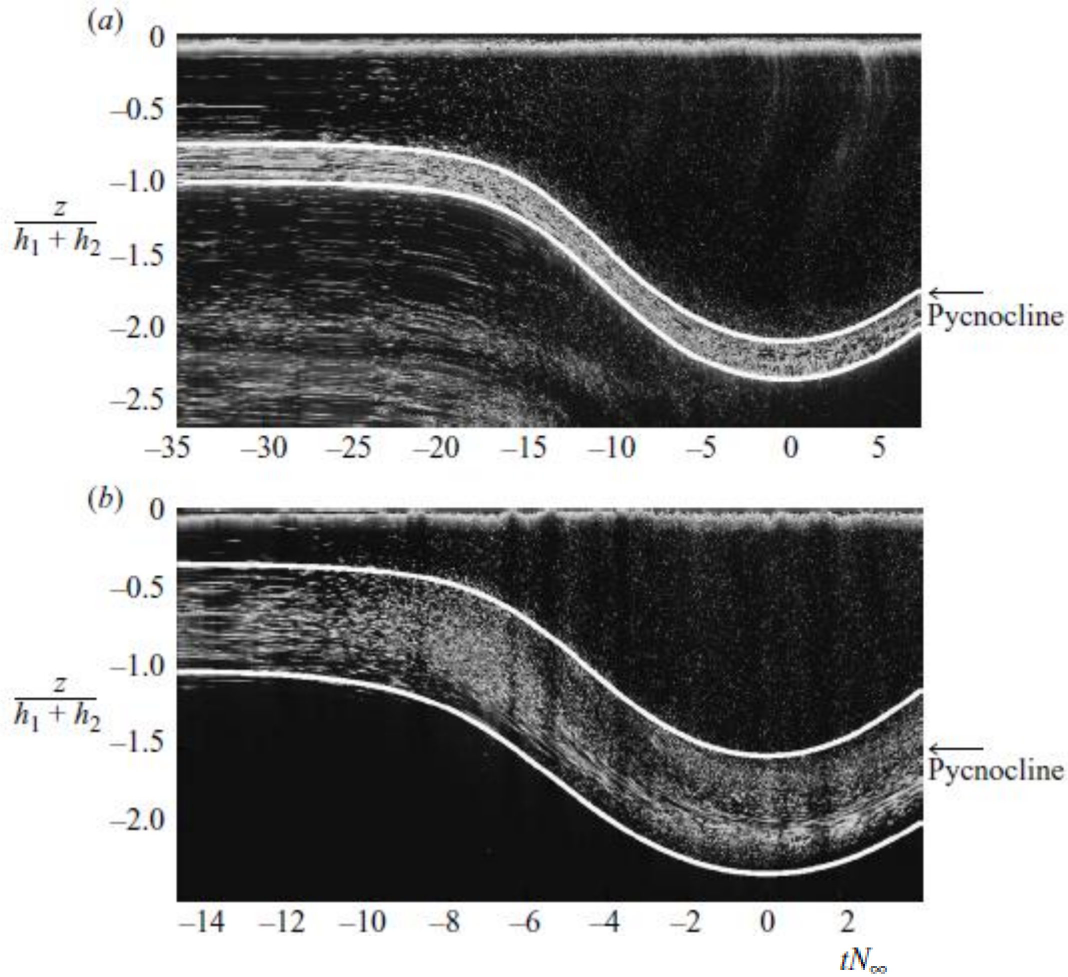

Fructus, Carr, Grue, Jensen & Davies (2009) JFM

Comparisons: lab data & theory

- Breaking

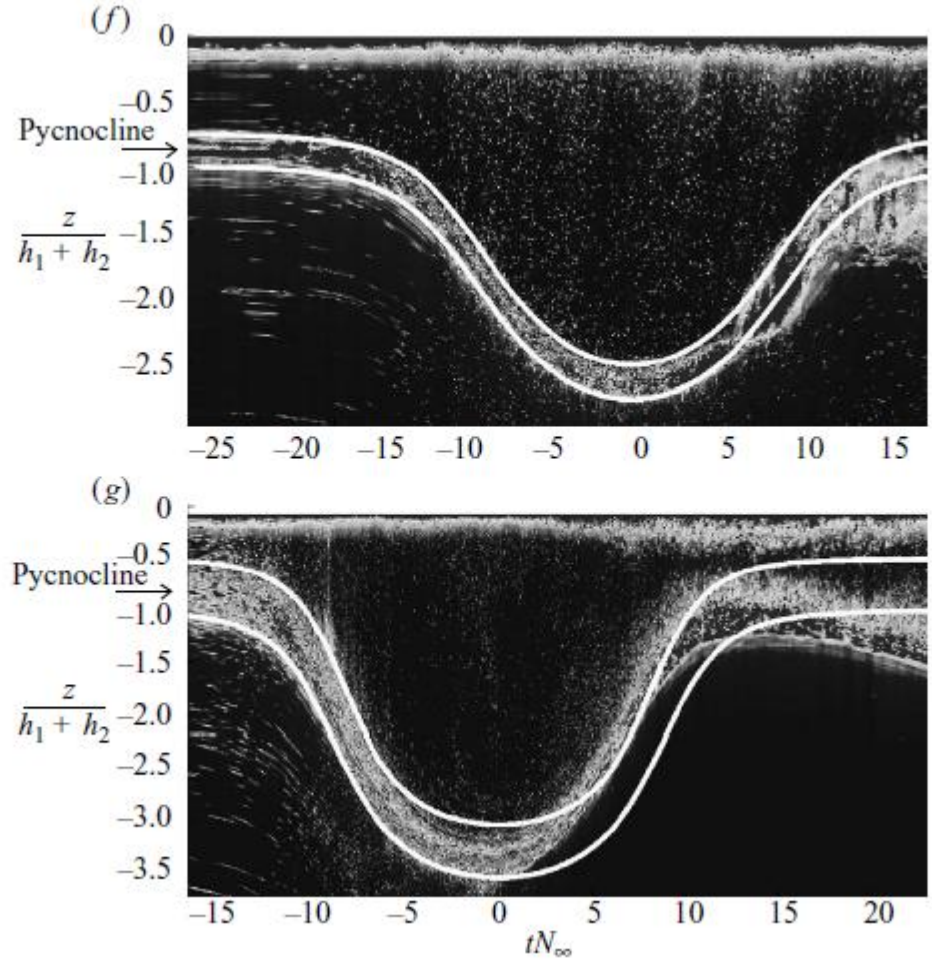

Fructus, Carr, Grue, Jensen & Davies (2009) JFM

Conditions for instability

- Define: $Ri_g = [g(\partial\rho/\partial z)]/[\rho_0(\partial u/\partial z)^2]$
- Linear stability condition (parallel shear flow): $Ri_g < (1/4)$

L_x/λ

Conditions for instability

- Define: $Ri_g = [g(\partial\rho/\partial z)]/[\rho_0(\partial u/\partial z)^2]$
- Linear stability condition (parallel shear flow): $Ri_g < (1/4)$

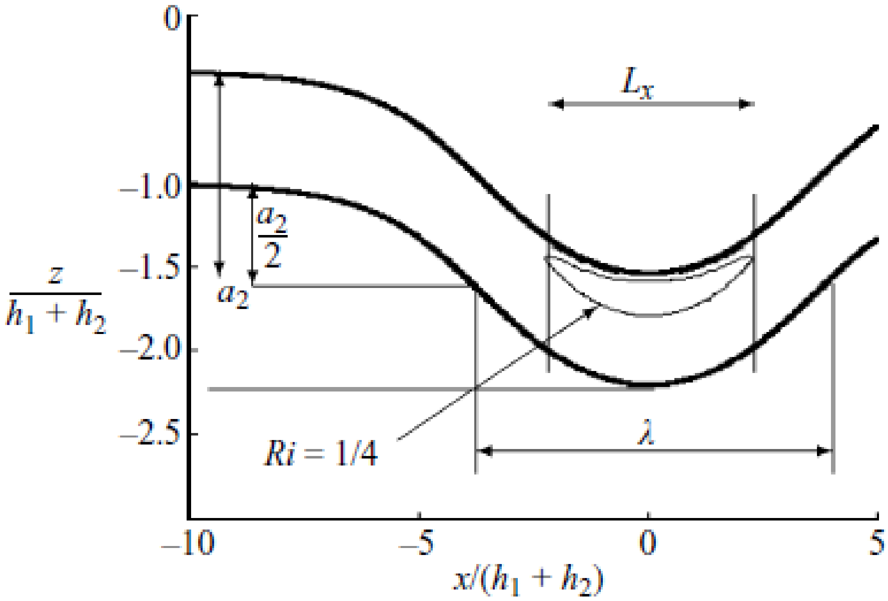

L_x/λ

Conditions for instability

- Define: $Ri_g = [g(\partial\rho/\partial z)]/[\rho_0(\partial u/\partial z)^2]$
- Linear stability condition (parallel shear flow): $Ri_g < (1/4)$

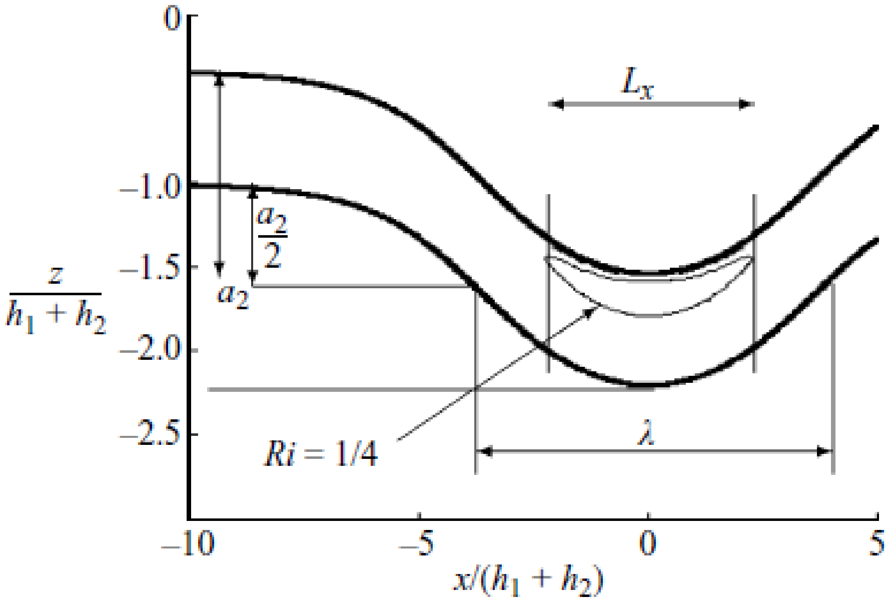

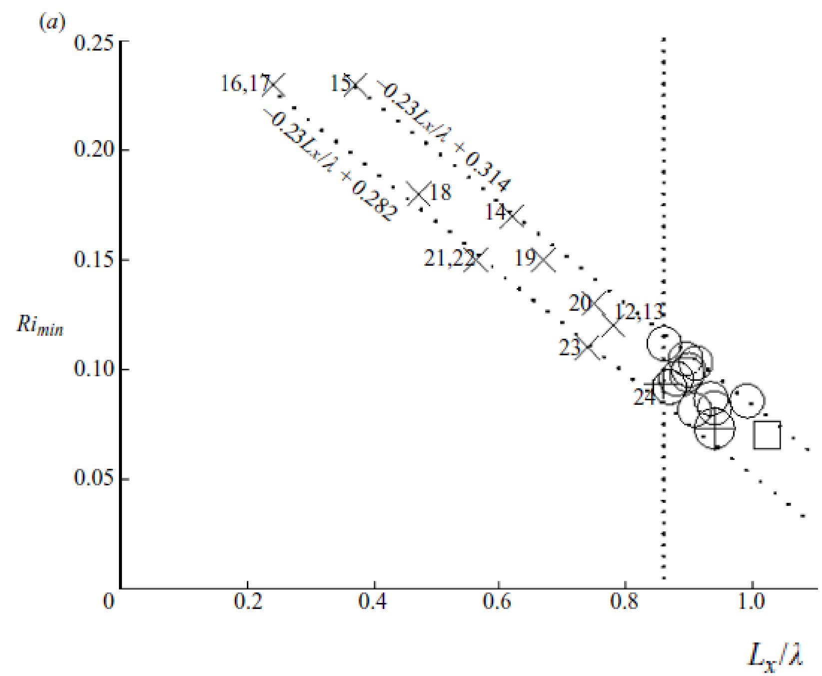

Breaking criterion: $L_x/\lambda > 0.86$

Mode-1: Breaking wave of depression

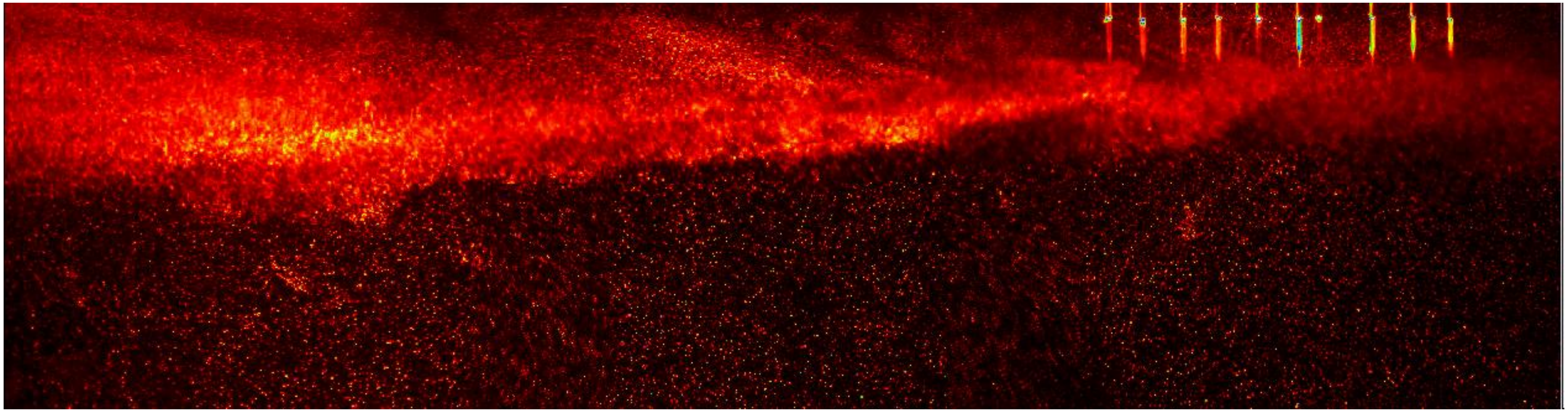

Oceanic observations: Mode 2 waves

- Mode 2 ISWs – S China Sea
- Yang *et al*., Nonlin. Proc in Geophys. (2010)

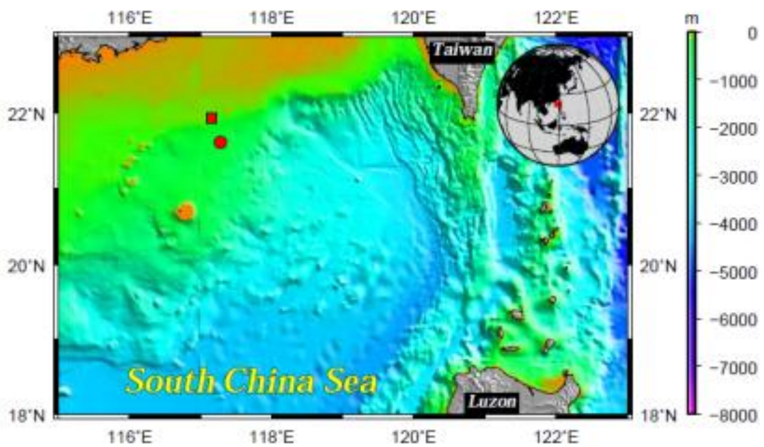

Fig. 1. The mooring location (shown as a red dot) on the continental slope of the northern South China Sea. The local water depth was 350 m. The square marks the location of the density profile in Fig. 4.

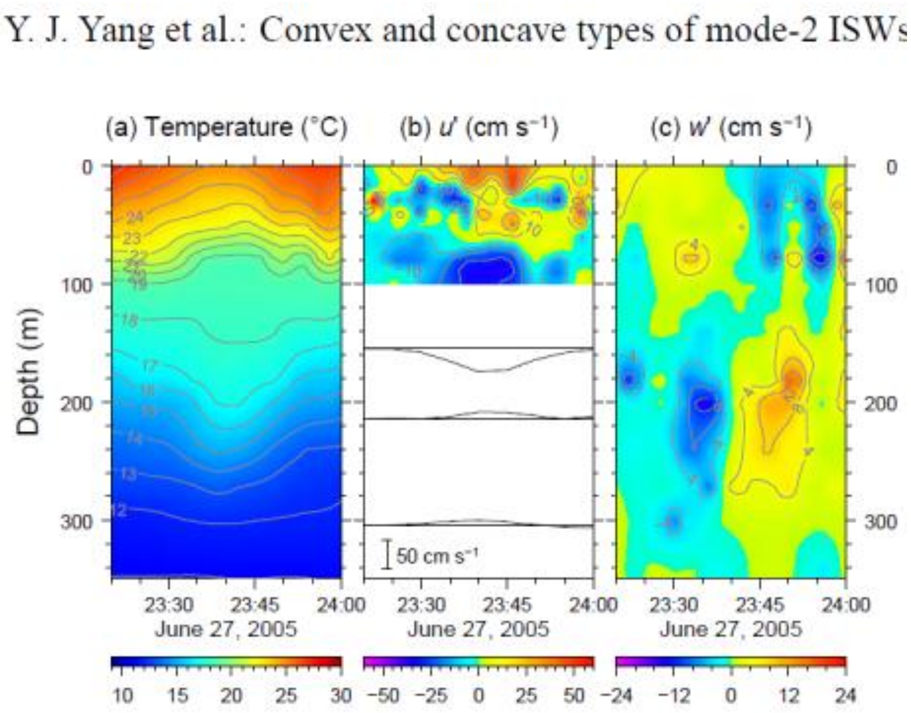

Mode 2: Present study (laboratory)

- (Carr, Davies & Hoebers, PoF, 2015)

- Inspired by recent numerical modelling studies
- Salloum, Knio & Brandt (2012)[1]
- Olsthoorn, Baglaenko & Stastna (2013)[2]

- Generation by release of mixed fluid into middle layer of a 3-layer, stably stratified fluid, either at mid-depth[1,2] or offset from mid-depth[2]

1. Numerical simulation of mass transport in internal solitary waves. Phys. Fluids 24, 016602 (2012)
2. Analysis of asymmetries in propagating mode-2 waves. Nonlin. Processes Geophys., 20, 59–69 (2013)

Salloum *et al* 2012

- Numerical model results: mass transport
- Continuation of Terez & Knio, JFM (1998)

56 D. E. Terez and O. M. Knio

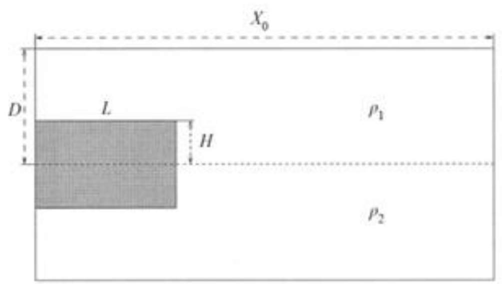

FIGURE 1. The initial configuration in the numerical simulations. Large-amplitude solitary waves are produced by a collapsing mixed region of height H and length L in a long, deep channel. The undisturbed density distibution in the channel is described by a hyperbolic tangent profile (2.1).

Release at mid depth
(0% offset)

Salloum *et al* 2012

- Numerical model results: mass transport
- Continuation of Terez & Knio, JFM (1998)

56 D. E. Terez and O. M. Knio

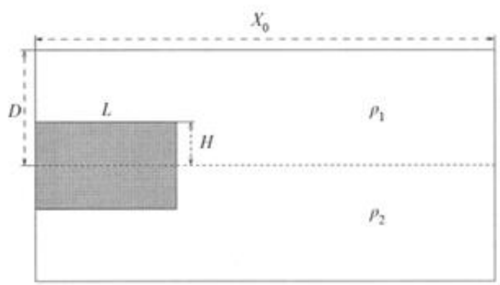

FIGURE 1. The initial configuration in the numerical simulations. Large-amplitude solitary waves are produced by a collapsing mixed region of height H and length L in a long, deep channel. The undisturbed density distibution in the channel is described by a hyperbolic tangent profile (2.1).

Release at mid depth
(0% offset)

Numerical simulations of large-amplitude internal solitary waves 61

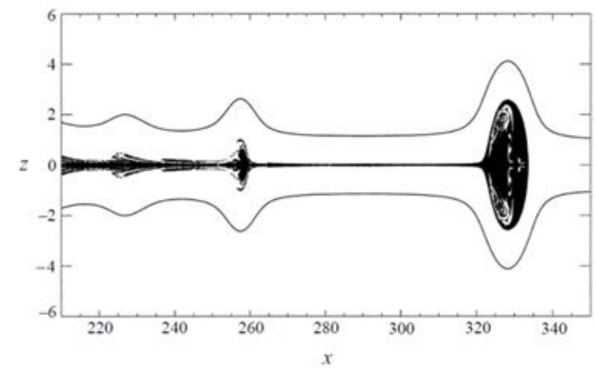

FIGURE 3. The train of large-amplitude solitary waves produced by the collapse of a mixed region with $H = 5$ and $L = 30$. The Reynolds number $Re = 50$ and the Schmidt number $Sc = 200$. The leading wave transports mixed fluid inside; it is followed by smaller waves, which can also transport fluid. The waves gradually separate in space as they propagate away from the origin.

Salloum *et al* 2012

- Numerical model results

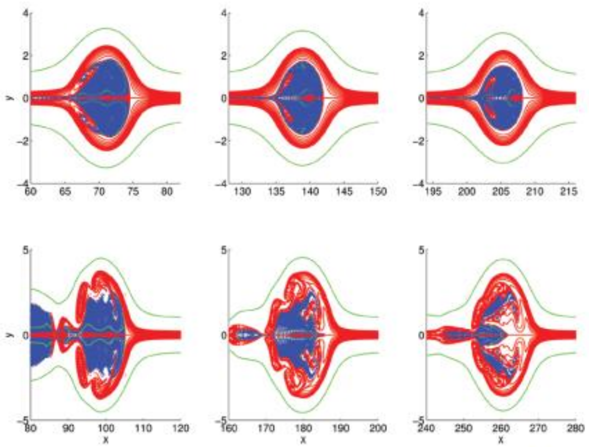

Fig. 5. (Color) Instantaneous distribution of Lagrangian particles contained inside and around the leading solitary wave. Top row: rectangular mixed region with $L = 10$ and $H = 4$. Bottom row: rectangular mixed region with $L = 30$ and $H = 5$. The plots are generated at $t = 35.1$ (left), $t = 70.2$ (middle), and $t = 105.3$ (right). In both cases, $Re = 100$. The blue color represents particles initially located in the mixed region; the red color represents particles located in the neighborhood of the pycnocline, and the green color represents particles originating at $y = \pm 1$.

Salloum *et al* 2012

- Numerical model results

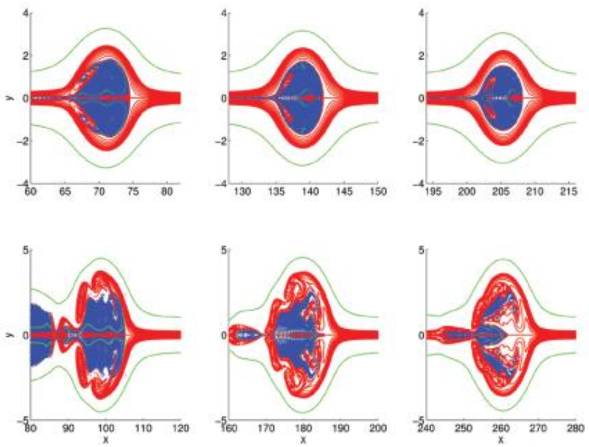

Fig. 5. (Color) Instantaneous distribution of Lagrangian particles contained inside and around the leading solitary wave. Top row: rectangular mixed region with $L = 10$ and $H = 4$. Bottom row: rectangular mixed region with $L = 30$ and $H = 5$. The plots are generated at $t = 35.1$ (left), $t = 70.2$ (middle), and $t = 105.3$ (right). In both cases, $Re = 100$. The blue color represents particles initially located in the mixed region; the red color represents particles located in the neighborhood of the pycnocline, and the green color represents particles originating at $y = \pm 1$.

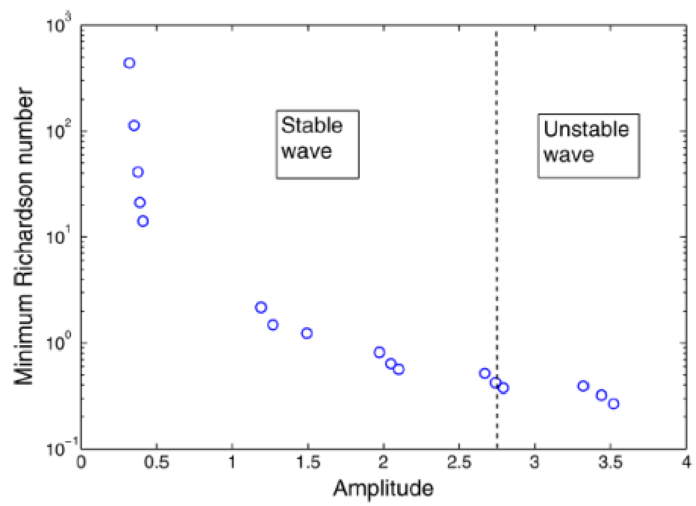

FIG. 14. (Color online) The minimum Richardson number within the leading wave versus the peak wave amplitude. The instability threshold ($Ri_{min} = 0.25$) is captured using the vertical dashed line.

Olsthoorn *et al* (2013)

- Numerical model results: Effects of offset (down ↓) from mid depth

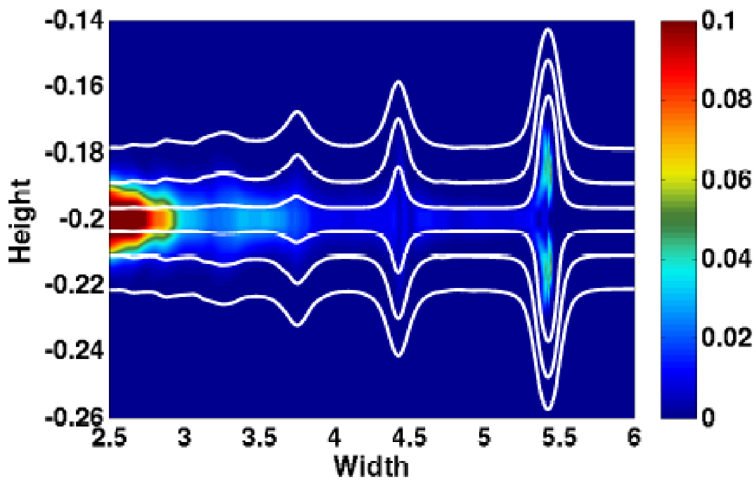

Fig. 4. Plot of the tracer concentration at $t = 100$ s for a initial mixed layer symmetric about a mid-depth pycnocline. The colorbar was saturated at 10 % of the maximum. Six contours of density are overlayed in order to identify the location of the internal waves. Notice that the distribution is entirely symmetric about the mid-depth. Three perfectly symmetric mode-2 waves are clearly observed.

Olsthoorn *et al* (2013)

- Numerical model results: Effects of offset (down ↓) from mid depth

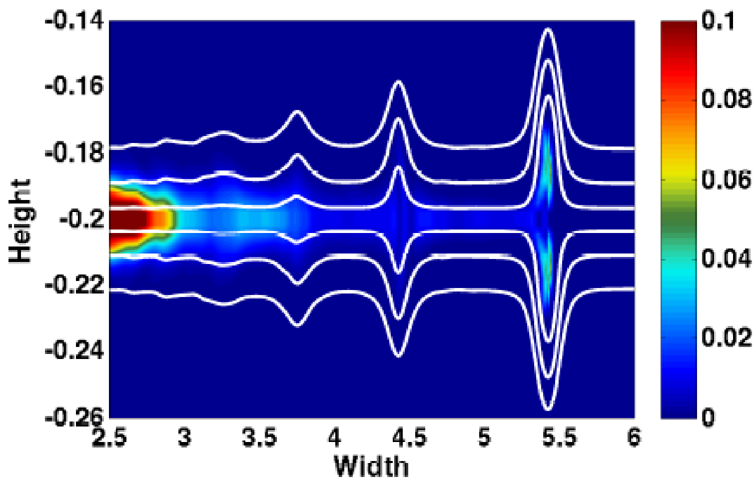

Fig. 4. Plot of the tracer concentration at $t = 100$ s for a initial mixed layer symmetric about a mid-depth pycnocline. The colorbar was saturated at 10 % of the maximum. Six contours of density are overlayed in order to identify the location of the internal waves. Notice that the distribution is entirely symmetric about the mid-depth. Three perfectly symmetric mode-2 waves are clearly observed.

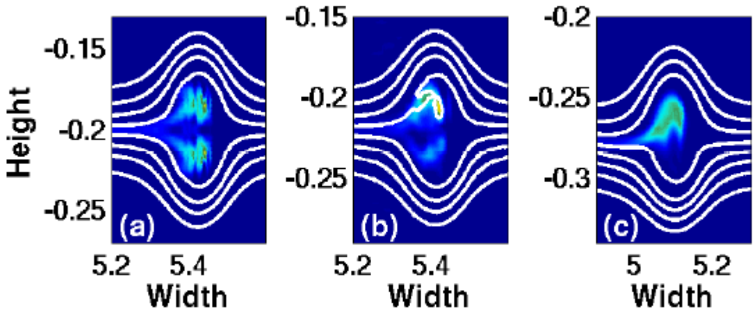

Fig. 6. A comparison of the largest mode-2 wave at time $t = 100$ s for a pycnocline centred at **(a)** $-z_0 = H/2$, **(b)** $-z_0 = H/2 + 0.05H$, and **(c)** $-z_0 = H/2 + 0.20H$. Eight isocontours of density are overlayed to depict the location of the mode-two wave. It is very clear the off-centre location of the pycnocline causes the tracer to lose its symmetry about the centre of the mode-2 wave. Colorbar is saturated to 10 % of its maximum value.

Laboratory system: present experiments

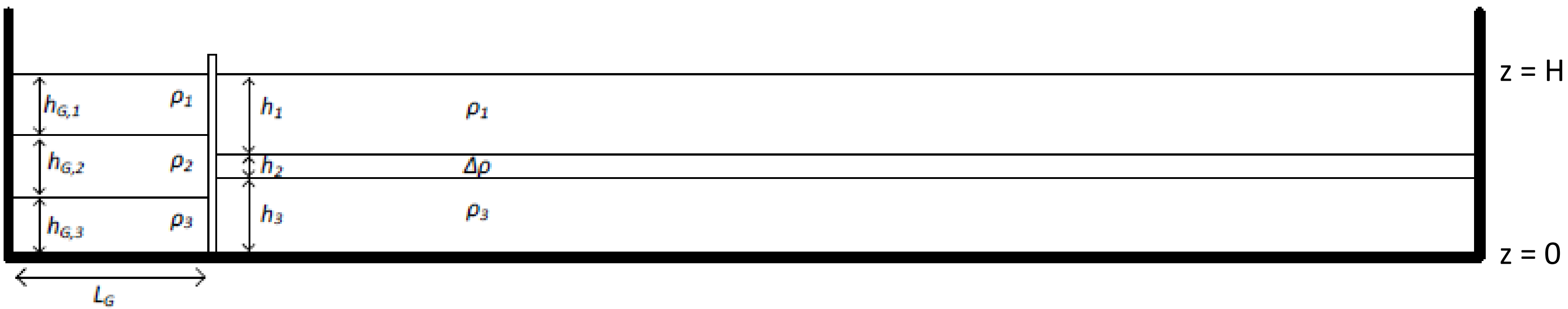

- Saline layers of density ρ_1, ρ_2, ρ_3, with $\rho_2 = (\rho_1 + \rho_3)/2$
- Tracer particles in working section only (*DigiFlow*)
- Density profiles with micro-conductivity sensors

Initial density configurations

- Case 1: zero offset
- (Salloum *et al*, 2012; Olsthoorn *et al*., 2013)

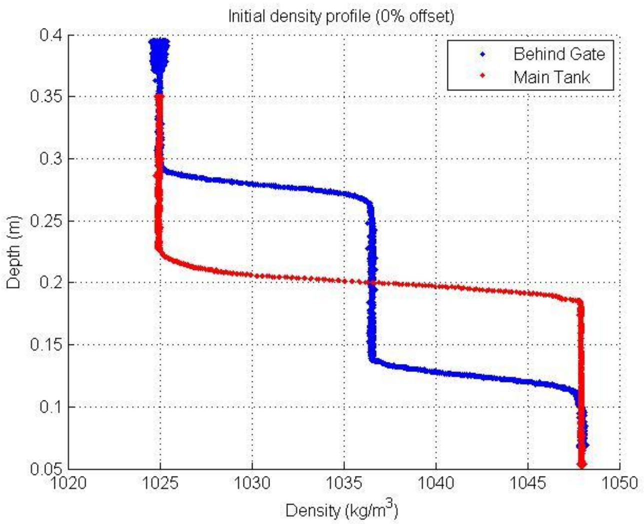

Initial density configurations

- Case 1: zero offset
- (Salloum *et al*, 2012; Olsthoorn *et al*., 2013)

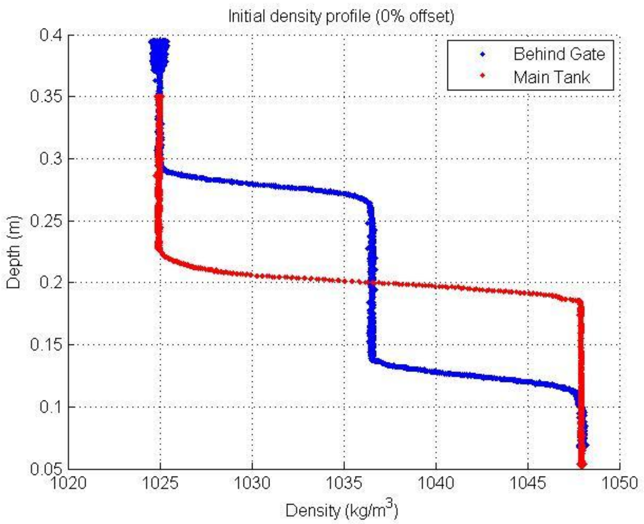

- Case 2: non-zero offset (20%)
- (Olsthoorn *et al*., 2013)

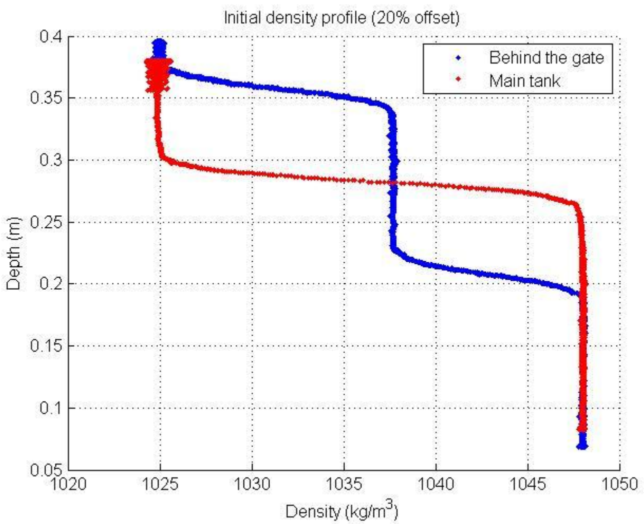

Olsthoorn *et al.*, 2013 case: 0% offset

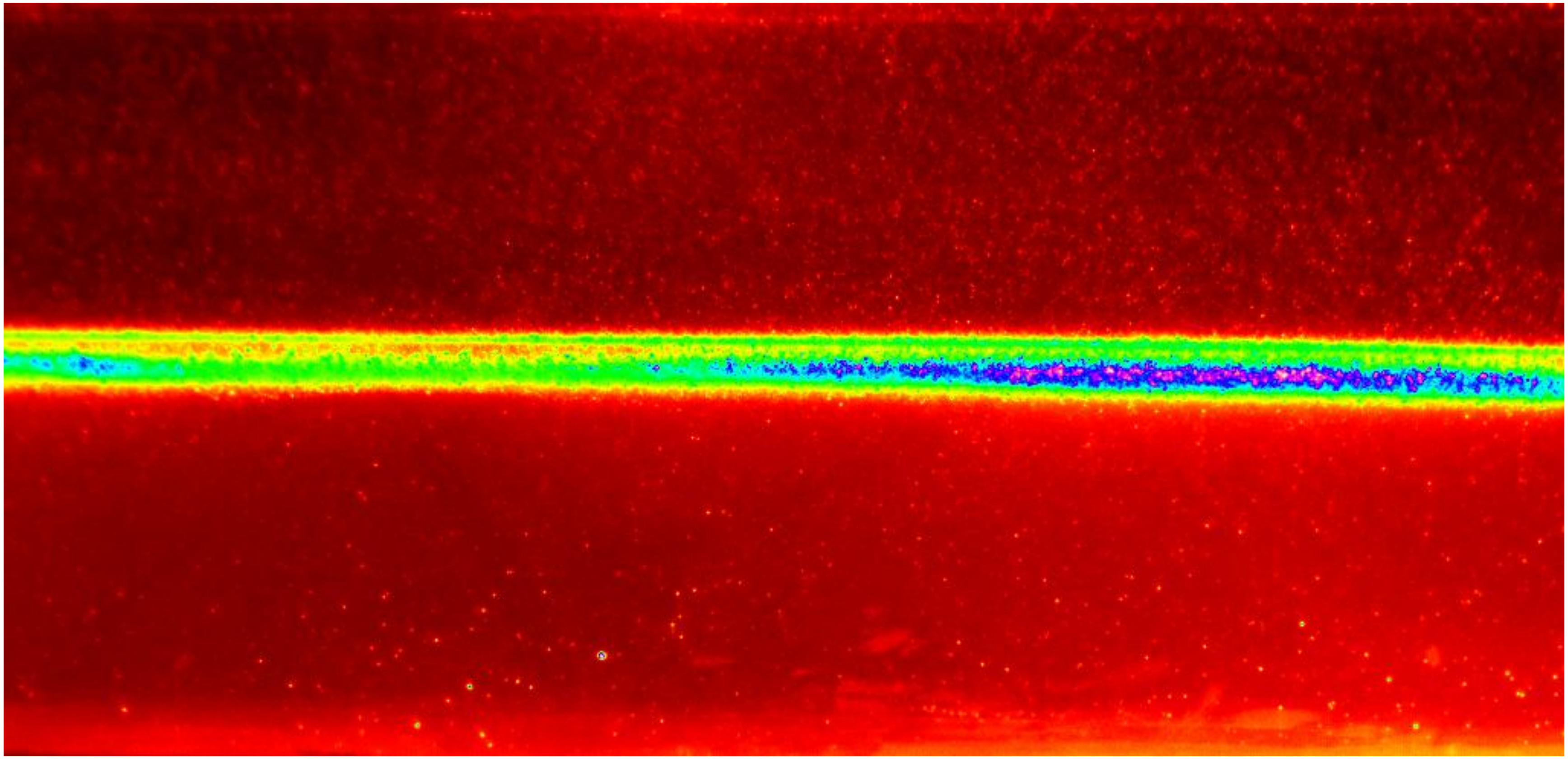

PIV data: 0% offset

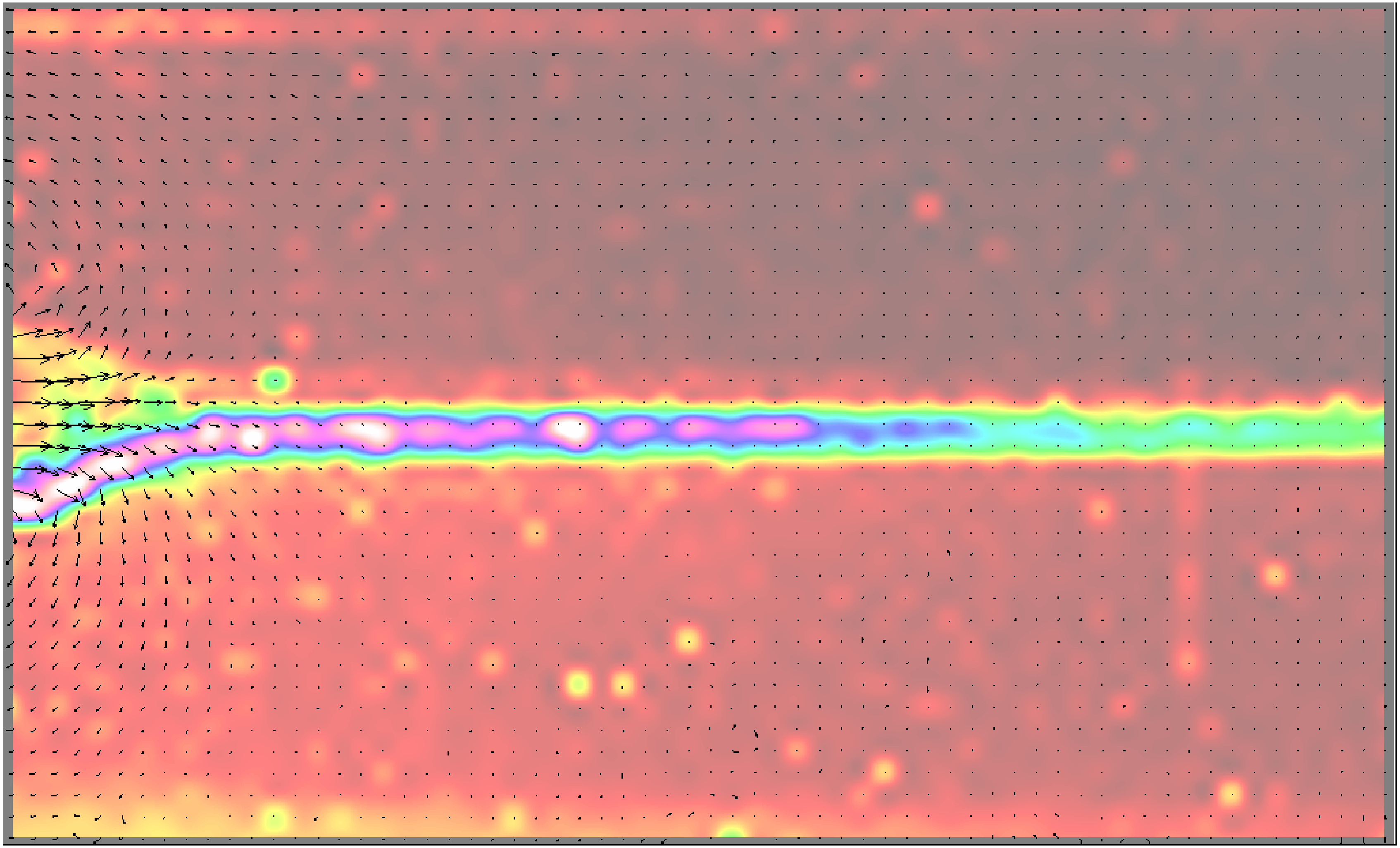

PIV data: 0% offset

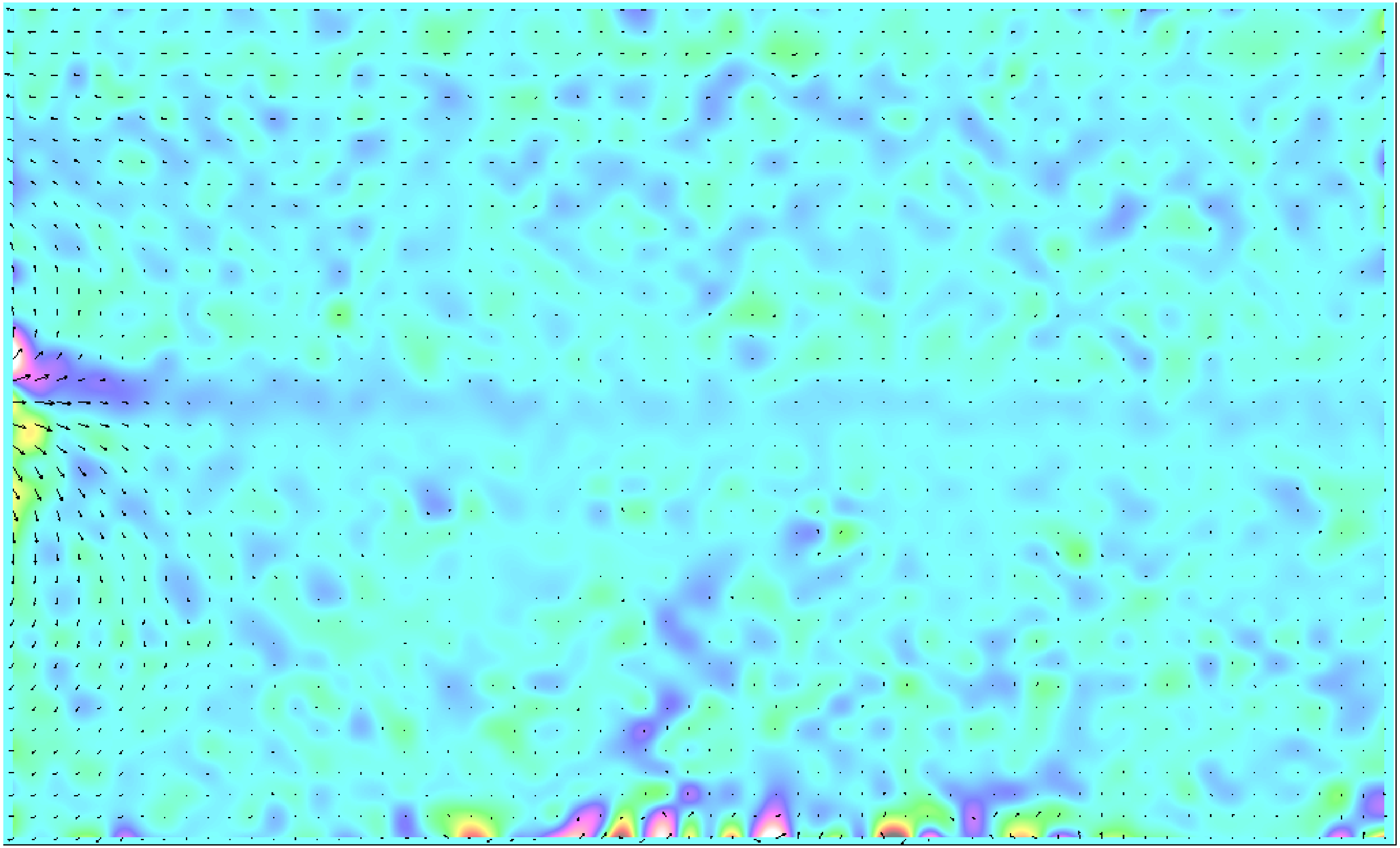

Olsthoorn *et al.*, 2013 case: 20% offset

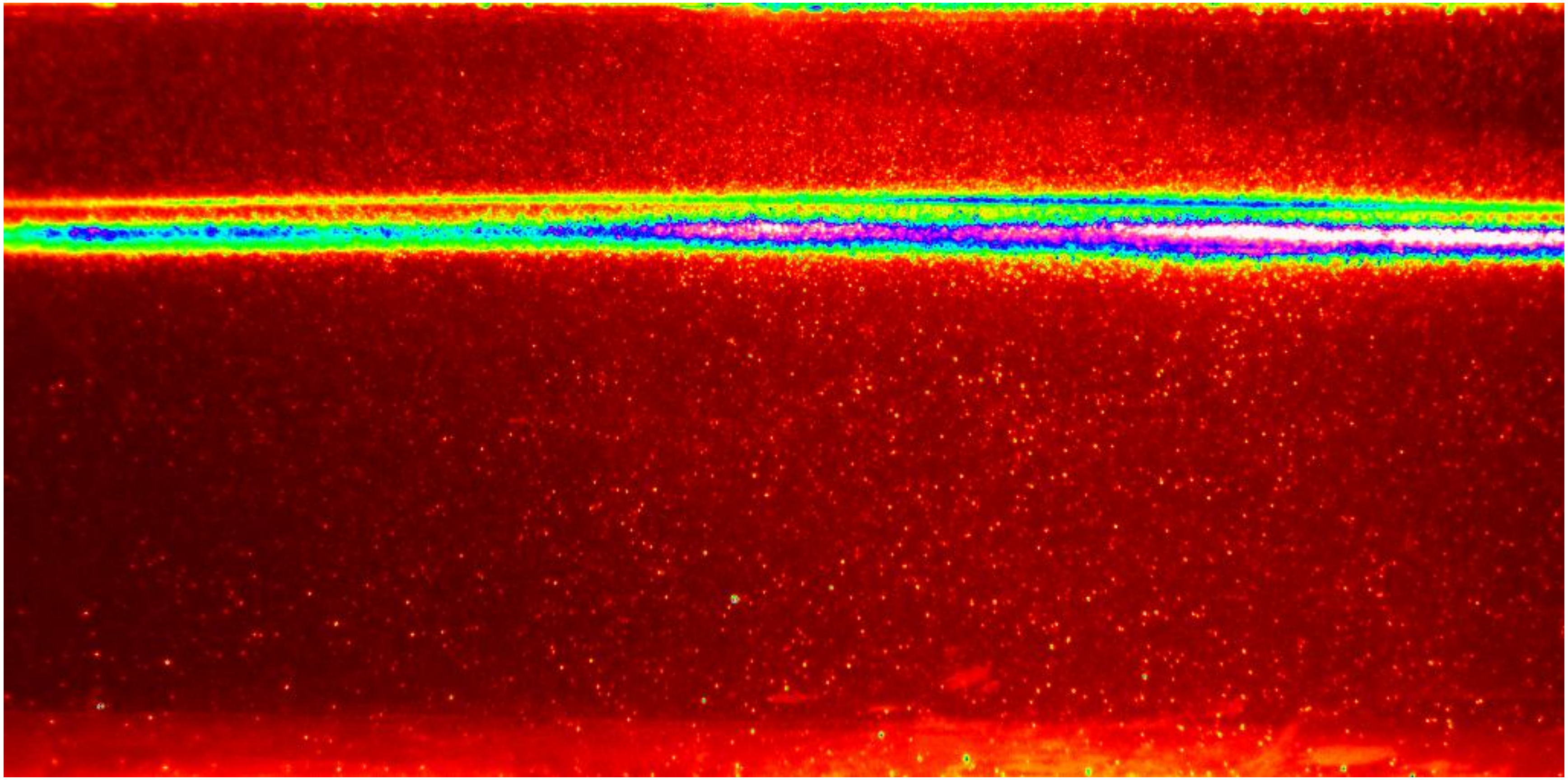

Olsthoorn *et al*., 2013 case: 0% offset, (unstable)

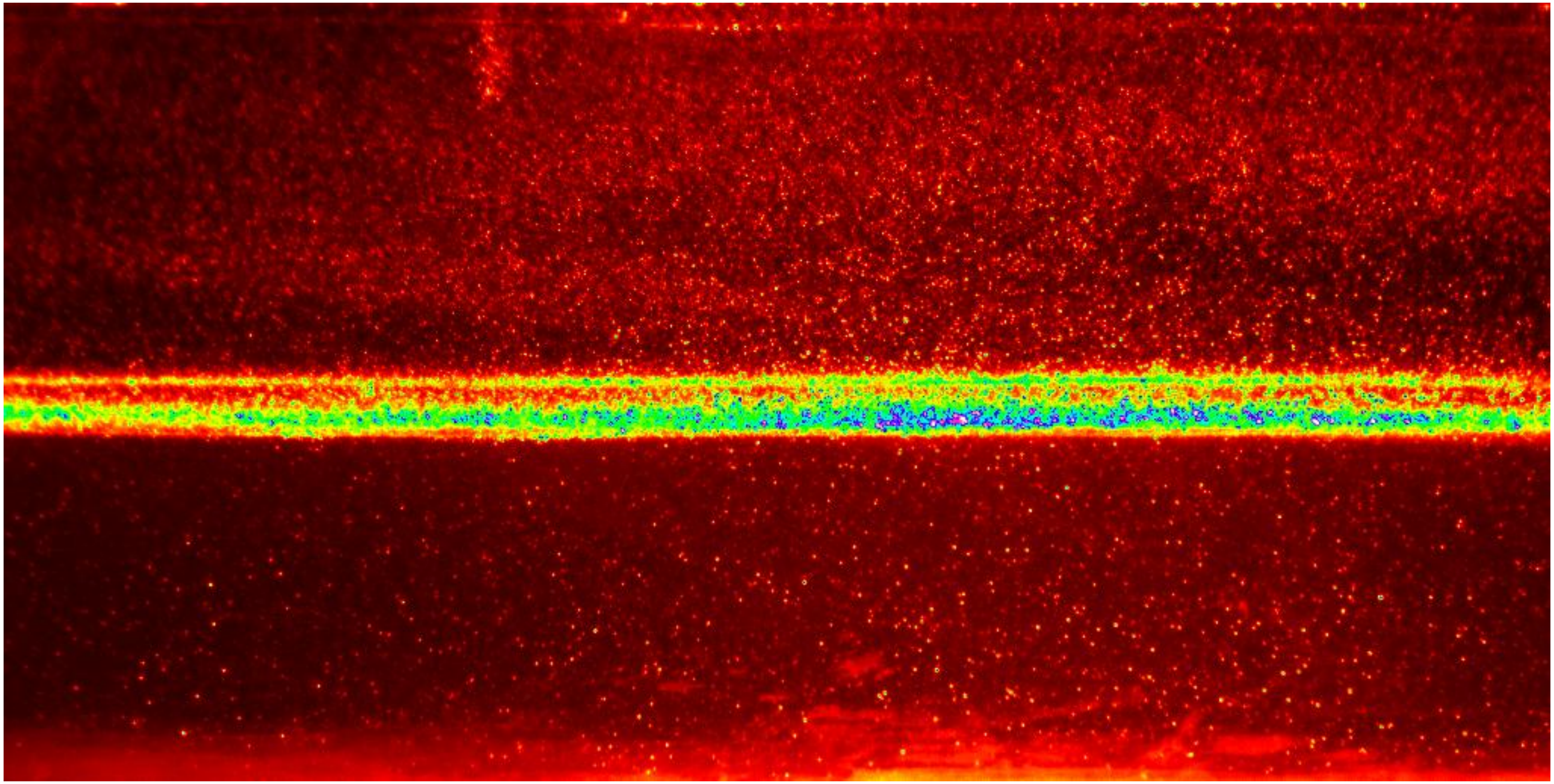

Olsthoorn *et al.*, 2013 case: 20% offset (unstable)

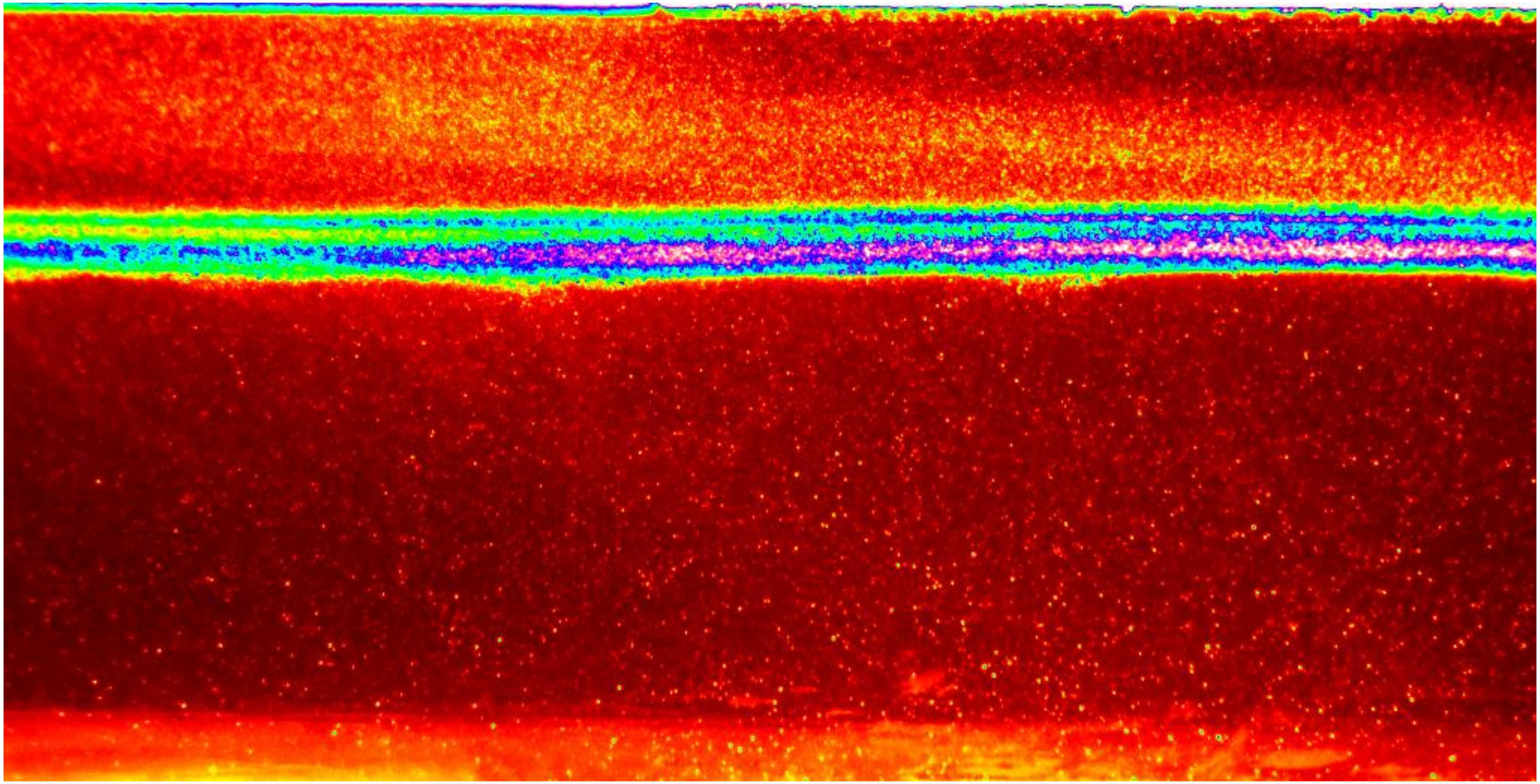

Time series data: Unstable waves

- Offset comparisons

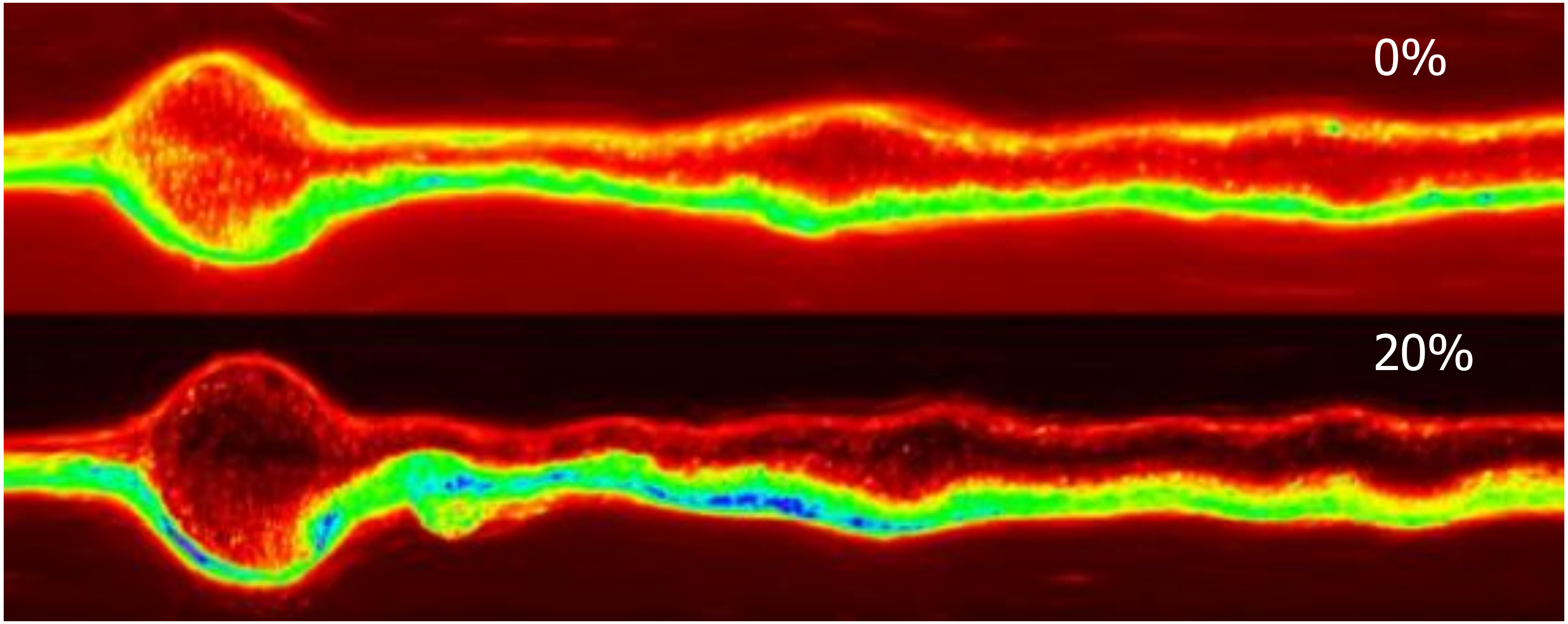

Comparison with Olsthoorn *et al* (2013)

- Stable Mode 2 waves: Peak spacing, amplitude decay

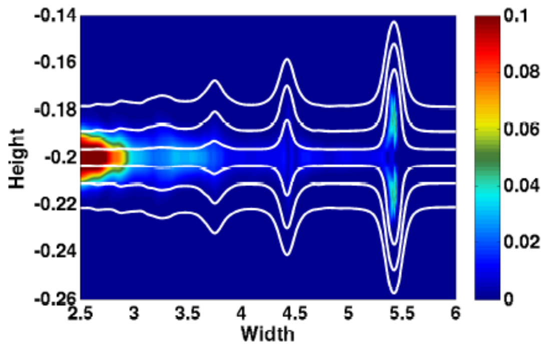

Fig. 4. Plot of the tracer concentration at $t = 100$ s for a initial mixed layer symmetric about a mid-depth pycnocline. The colorbar was saturated at 10 % of the maximum. Six contours of density are overlayed in order to identify the location of the internal waves. Notice that the distribution is entirely symmetric about the mid-depth. Three perfectly symmetric mode-2 waves are clearly observed.

0% offset case

	x_1 (m)	x_2 (m)	x_3 (m)	a_1 (m)	a_2 (m)	a_3 (m)
Numerical	5.40	4.42	3.75	0.0346	0.0213	0.0106
Laboratory	5.40	4.60	4.10	0.0330	0.0170	0.0060

Breaking wave: 20% offset

4 3 2 1

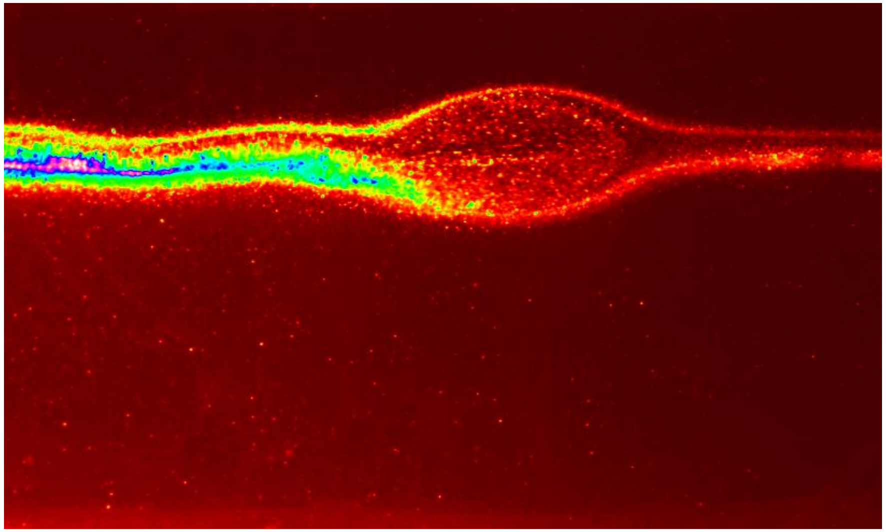

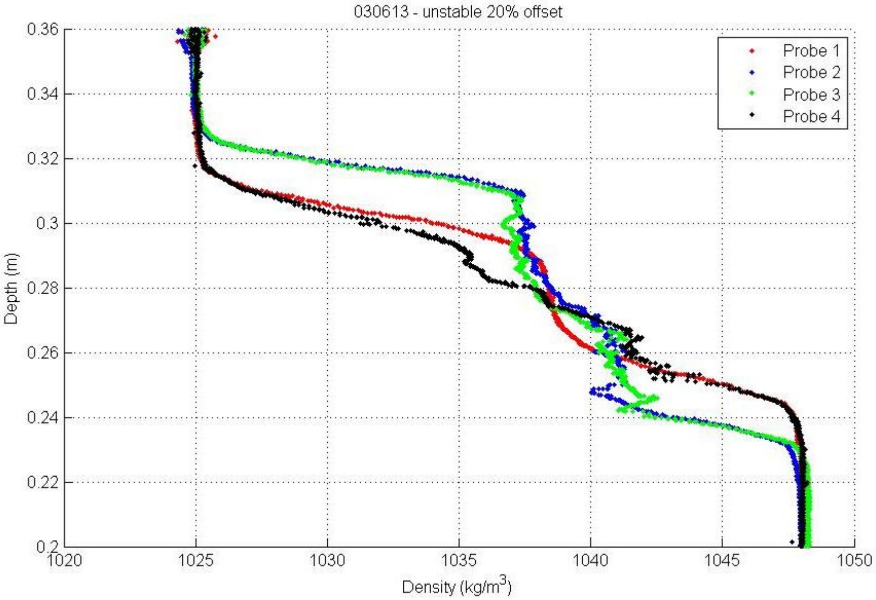

030613

Conclusions

- Good understanding of Mode 1 dynamics, for internal solitary waves
- Need for further studies of vertical mixing, sediment re-suspension for Mode 1 waves
- Preliminary experiments with Mode 2 waves agree qualitatively with Olsthoorn *et al* (2013), Salloum *et al* (2012)
- For 0% offset, mode 2 wave pattern and amplitude decay data in good agreement with Olsthoorn *et al* (2013) for stable waves
- As pycnocline offset increases, Mode 2 wave develops asymmetry, skewness about vertical.
- Critical amplitude for shear instability is function of offset.